Turkish Journal of Physics

Volume 49 | Number 3 Article 4

6-25-2025

Evolution of wormholes under f(R, T) theory, the Karmarkar condition and the Casimir energy

MURAT METEHAN TÜRKOĞLU

Follow this and additional works at: https://journals.tubitak.gov.tr/physics

 Part of the Physics Commons

Recommended Citation

TÜRKOĞLU, M. M (2025). Evolution of wormholes under f(R, T) theory, the Karmarkar condition and the Casimir energy. *Turkish Journal of Physics 49* (3): 92-122. https://doi.org/10.55730/1300-0101.2778



This work is licensed under a Creative Commons Attribution 4.0 International License.
This Research Article is brought to you for free and open access by TÜBİTAK Academic Journals. It has been accepted for inclusion in Turkish Journal of Physics by an authorized editor of TÜBİTAK Academic Journals. For more information, please contact academic.publications@tubitak.gov.tr.

TÜBİTAK

Turkish Journal of Physics

http://journals.tubitak.gov.tr/physics/

Research Article

Turk J Phys
(2025) 49: 92 – 122
© TÜBİTAK
doi:10.55730/1300-0101.2778

Evolution of wormholes under $f(R,T)$ theory, the Karmarkar condition and the Casimir energy

Murat Metehan TÜRKOĞLU[1,2,*]

[1]Department of Aeronautical Engineering, İstanbul Gelişim University, İstanbul, Turkiye
[2]Graduate School, Defense Technologies, Aeronautics and Astronautics Engineering Program, İstanbul Technical University, İstanbul, Turkiye

Received: 30.12.2024 • **Accepted/Published Online:** 28.05.2025 • **Final Version:** 25.06.2025

Abstract: In this study, both the evolution of wormholes (by examining both the energy conditions and using the TOV equations) and the effects of the Karmarkar condition on the solutions obtained under certain specific cases were examined in the light of the $f(R,T)$ gravity theory, using two $f(R,T)$ functions predicted to describe the accelerated expansion of the universe. In this context, for the first time in the literature, a generalized shape function was obtained using the Karmarkar condition. It was observed that solutions of the type $R-a_1^2/R+a_2g(T)$ satisfy the energy conditions (with the dominant energy condition being partially satisfied), whereas solutions of the type $R+a_1^2R^2+a_2g(T)$ require the presence of exotic matter. In both cases, stable, static, and traversable wormhole solutions were obtained. By applying the Karmarkar condition to the $R+a_1^2R^2+a_2g(T)$ type solutions, which violate the energy conditions, the relationship between wormhole geometry and energy conditions was investigated. The study examined whether the Karmarkar condition eliminates the need for exotic matter, and it was found that the solutions do not remove the necessity of exotic matter. Additionally, it was demonstrated that a specific value of the parameter, β, which determines the radial variation of the shape function, could ensure the stability of the wormhole throat with the aid of Casimir energy. In other words, it is considered possible that the geometric evolution of the wormhole throat could trigger the transition from positive energy (baryonic matter) to negative energy (dark matter, dark energy, or other exotic matter) by inducing Casimir forces.

Key words: $f(R,T)$ gravity, wormhole, energy conditions, Karmarkar condition, Casimir wormholes, equation of states

1. Introduction

Wormholes can be thought of as topological bridges that are hypothesized to connect distant regions of the universe or different universes, emerging as solutions to Einstein's field equations. The first scientific analysis of wormholes was conducted in 1916 by Flamm, who examined the Schwarzschild solution, one of the newly discovered solutions of general relativity at that time [1]. Subsequently, in 1935, modern wormhole solutions were introduced by Einstein and Rosen (ER), who proposed a model in which different regions of space are connected through a "bridge." This model is now known as the Einstein-Rosen bridge [2]. The reason for the popularity of wormholes is that they have been

*Correspondence: mmturkoglu@gelisim.edu.tr

This work is licensed under a Creative Commons Attribution 4.0 International License.

conceptualized as a type of "time machine." In this sense, Morris and Thorne [3] analyzed wormholes as traversable time machines, contributing to their modern popularity. The most important feature that wormholes must satisfy to be traversable is that the gravitational tidal forces acting on a person traveling in a spacecraft remain within reasonable limits. Additionally, geometrically, wormholes must satisfy the condition known as flaring-out, which imposes a boundary condition on the minimum throat radius. However, this condition is incompatible with the null energy condition (NEC), which states that an observer must measure a nonnegative average energy density in spacetime. The violation of the NEC requires the existence of exotic matter, and modified theories of gravity have been invoked to obtain physically consistent wormhole solutions. For example, Armendariz-Picon showed that the NEC is satisfied in the presence of a massless scalar field and that the Einstein equations provide nonsingular, traversable wormhole geometries [4]. Sushkov obtained exact solutions for a static, spherically symmetric wormhole with phantom energy and demonstrated that the spatial distribution of the phantom energy is confined to the throat region of the wormhole [5]. Additionally, other studies in the literature where similar results have been obtained can be reviewed [6, 7]. Furthermore, exact solutions of spherically symmetric wormholes supported by generalized Chaplygin gas (GCG) have also been explored in the literature [8]. (For a more comprehensive review, the following references are recommended for further study: [9–14]).

The question of whether exotic matter fields are necessary for the traversability of wormholes is significant. In this context, it is examined whether the solutions of the field equations, obtained by adding the trace of the energy-momentum tensor to the gravitational Lagrangian in $f(R,T)$ gravity, eliminate the need for exotic matter [44, 45]. In their study, Deng and Meng [15] examined the structure and topology of wormholes in the presence of dark energy. In the Einstein-Dirac-Maxwell theory, traversable, asymptotically flat wormhole solutions that are free from singularities and exotic matter were obtained using massive fermions [16]. Additionally, another method for obtaining wormholes without exotic matter is the application of the thin-shell approximation [17, 18]. Moreover, it has been demonstrated in Brans-Dicke gravity that exotic matter is not required to support the throat geometry of wormholes [46, 47].

There are many studies examining wormholes within the framework of modified theories of gravity, $f(R,T)$ gravity. [19–29, 31–43, 48–55]. Additionally, recent studies have yielded highly significant results. For example, Ganiyeva et al. presented a wormhole solution that satisfies all energy conditions without requiring fine-tuning [62]. Roy et al. demonstrated that within the framework of the f(R,T) theory, evolving and traversable wormhole solutions that violate the NEC condition but do not require exotic matter are possible [63]. Yousaf and Asad used Visser's cut-and-paste technique to construct thin-shell wormholes and revealed that minimally coupled f(R,T) gravity models support various wormhole configurations [64]. Bhatti et al. discussed the junction using distribution formalism and examined the isotropic perfect fluid, as well as the polytropic equation of state that supports exotic matter at the throat of the shell [65]. Rastgoo and Parsaei presented wormhole solutions with an asymptotically linear equation of state and proved that their solutions satisfy all energy conditions [66]. Chaudhary et al. obtained stable and traversable wormhole solutions supported by exotic matter using specific shape functions [67]. Lu et al. obtained wormhole solutions that satisfy all energy conditions without the need for exotic matter or any specific type of matter, using a specially chosen f(R,T) function [68]. Tangphati et al. showed that within the framework of f(R,T) theory, the wormhole energy density is always positive, while the radial pressure is negative. They have stated

that this result indicates the necessity of exotic matter for the existence of wormholes [69]. Yashwanth et al. demonstrated that within the framework of f(R,T) theory, Finslerian wormhole models require exotic matter to maintain the stability of the wormhole throat [70]. Mondal and Rahaman studied wormholes within the framework of f(R,T) gravity theory using the Navarro–Frenk–White (NFW) density profile, the universal rotation curve (URC) dark matter profile, and the mass density profile. They showed that some special wormhole solutions may exist without requiring the presence of exotic matter [71]. Azmat et al. examined the Casimir energy densities generated between two parallel plates, a cylinder, and a sphere, and compared them with the f(R,T) field equations. They demonstrated that exotic matter is required for the stability of wormholes [72]. Chaudhary et al. examined various cases of wormholes supported by phantom fluid within the framework of f(R,T) theory. They showed that the first type of phantom solutions violate the radial null energy condition (NEC), while the tangential NEC is satisfied. On the other hand, they proved that the second type of wormhole solutions violate the NEC [73].

The most important feature of the $f(R,T)$ theory is that it explains the observed expansion of the universe without resorting to dark matter and dark energy [49]. In this study, cosmological models of the type $R-a_1^2/R+a_2g(T)$ and $R+a_1^2R^2+a_2g(T)$ are discussed in detail. The main motivation of the paper is to predict the behavior of fundamental physical quantities (energy density, radial and tangential pressure) describing the evolution of a wormhole using f(R,T) functions, which are proposed to characterize the late-time acceleration of the universe, and to determine under which conditions wormholes require the presence of exotic matter. Based on the assumption that the wormhole geometry influences its evolution, the study investigates whether changes in the geometry can trigger transitions from baryonic matter to exotic matter (or vice versa).

We fix the speed of light and the gravitational constant via $c=G=1$. Throughout this work, a unitless value r/M is assigned by normalizing the radial coordinate r with respect to M (mass of wormhole), so that valid results can be produced for any value of M (see [22]).

2. Wormhole geometry

In this study, we focus on a spherically symmetric and static wormhole model. The general spherically symmetric and static wormhole metric is given in spherical coordinates, (t,r,θ,ϕ), as follows,

$$ds^2=-e^{\delta(r)}dt^2+\left[1-\frac{b(r)}{r}\right]^{-1}dr^2+r^2d\Omega^2, \tag{2.1}$$

where $\delta(r)$ is the redshift function, $b(r)$ is the shape function, and $d\Omega^2=d\theta^2+\sin^2\theta d\phi^2$ is the surface-element on the two-sphere. The traversability of the wormhole depends on the functions $\delta(r)$ and $b(r)$ satisfying several conditions. For instance, a spacetime traveler must be able to pass through the wormhole throat at $r=r_0$. For this, there should be no event horizon in the spacetime. This condition is fulfilled if the redshift function remains finite throughout the entire spacetime, in other words, $|\delta(r)|<\infty$. The second condition is known as the flaring-out condition, which ensures that the wormhole throat has a minimum size.

$$b(r_0)=r_0, \qquad b'(r_0)<1. \tag{2.2}$$

The redshift function and shape function that satisfy the conditions above have been chosen as follows [23]:

$$\delta(r) = \delta_0 \left(\frac{r_0}{r}\right)^{\alpha}, \tag{2.3}$$

$$b(r) = b_0 \left(\frac{r_0}{r}\right)^{\beta}, \tag{2.4}$$

where δ_0, α, and β are constants, and for the solutions to be physically acceptable (to ensure asymptotic flatness), α and β must be chosen as positive. We can analyze the topology of a traversable wormhole through its embedding in three-dimensional Euclidean space. To comply with spherical symmetry, we can choose $\theta = \pi/2$, and since we assume the wormhole to be static, we can set the time as constant. In this case, the line element is obtained as follows,

$$ds^2 = \frac{dr^2}{1 - b/r} + r^2 d\phi^2. \tag{2.5}$$

The surface described by Equation (2.5) can be represented using the cylindrical metric defined in terms of the three-dimensional cylindrical coordinates (r, ϕ, z).

$$ds^2 = dz^2 + dr^2 + r^2 d\phi^2. \tag{2.6}$$

Equation (2.6) can be rewritten as:

$$ds^2 = \left[1 + \left(\frac{dz}{dr}\right)^2\right] dr^2 + r^2 d\phi^2, \tag{2.7}$$

where

$$dz = \frac{dz}{dr} dr. \tag{2.8}$$

Using (2.5) and (2.7), we get

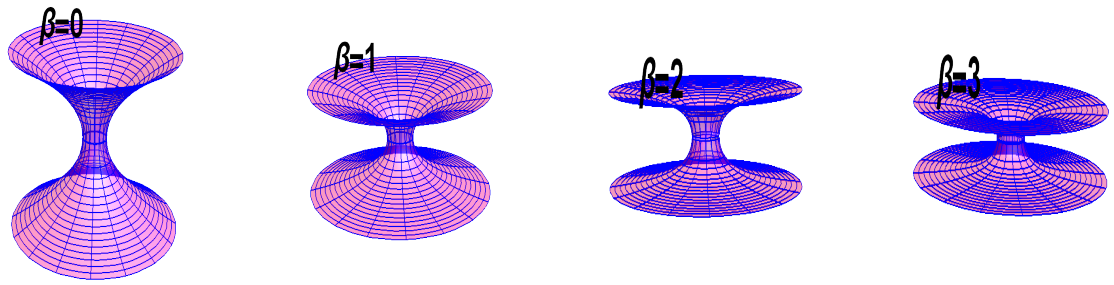
$$\frac{dz}{dr} = \pm \left(\frac{r}{b} - 1\right)^{-1/2}, \tag{2.9}$$

Here, since the wormhole has a minimum radius, as $r \to b_0$, we find that $dz/dr \to \infty$. Additionally, to obtain an asymptotically flat solution, as $r \to \infty$, both $b/r \to 0$ and $\delta \to 0$ must hold.

Using the shape function, the embedding function can be found as follows:

$$z(r) = i r_2 F_1 \left(\frac{1}{2}, \frac{1}{1+\beta}, 1 + \frac{1}{1+\beta}, (r/b_0)^{1+\beta}\right) \\ -i/b_0 \sqrt{\pi} \frac{\Gamma(1 + \frac{1}{1+\beta})}{\Gamma(\frac{1}{2} + \frac{1}{1+\beta})}, \tag{2.10}$$

where ${}_2F_1(\alpha, \beta, \gamma, t)$ is the hypergeometric function. The evolution of the wormhole topology depending on different values of β for $r_0 = 1$ is shown in Figure 1. The variation of the function $z(r)$ for different β values is shown in Figure 2.



(a) (b) (c) (d)

Figure 1. Embedding diagram for different β values according to Eq. (2.10). The throat radius has been set to $r_0 = 1$.

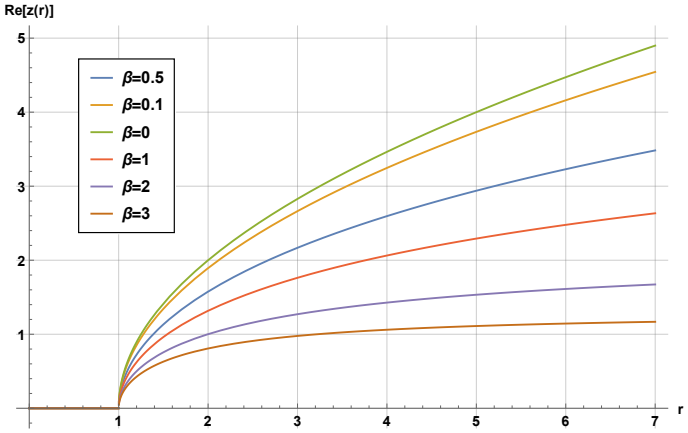


Figure 2. The behavior of the function $z(r)$ for different values of β with $b_0 = 1$.

According to Morris and Thorne [3], for wormholes to be traversable, the shape function must satisfy the following conditions:

- At the throat: $r = b(r)$ at $r = r_o$.
- The essential condition $\frac{b(r)-rb'(r)}{b(r)^2} > 0$ must be satisfied at $r = r_o$.
- $b(r)$ must satisfy $b'(r) < 1$.
- asymptotically flat space-time geometry condition, $\frac{b(r)}{r} \to 0$ as $r \to \infty$.

The behavior of the conditions that the shape function must satisfy is shown in Figure 3.

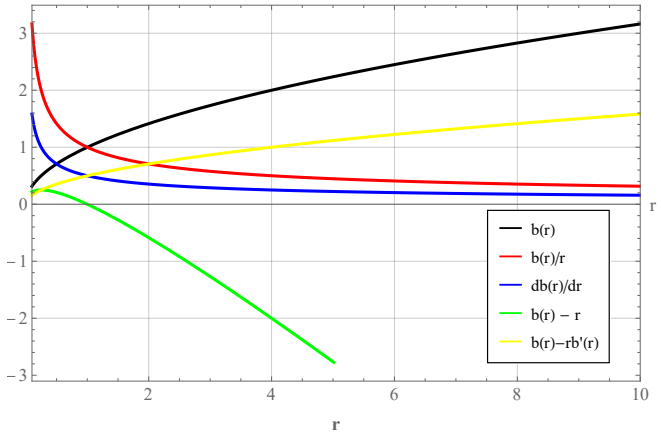


Figure 3. Evaluation of wormhole shape function $b(r)$ for $r_0 = 1$.

3. $f(R,T)$ field equations

The $f(R,T)$ action is given as [49]

$$S = \int d^4x\sqrt{-g}\left[\frac{1}{16\pi}f(R,T) + L_m\right], \tag{3.1}$$

where g is the determinant of the metric $g_{\mu\nu}$ and L_m the matter Lagrangian.

If we take the variation of the above action with respect to the metric, we obtain the field equations as shown below:

$$f_R R_{\mu\nu} - \frac{1}{2}f(R,T)g_{\mu\nu} + (g_{\mu\nu}\nabla^\mu\nabla_\nu - \nabla_\mu\nabla_\nu)f_R = 8\pi T_{\mu\nu} + f_T(T_{\mu\nu} - L_m g_{\mu\nu}), \tag{3.2}$$

where $f_R \equiv \partial f(R,T)/\partial R$, $R_{\mu\nu}$ is the Ricci tensor, $T_{\mu\nu}$ is the energy-momentum tensor, and $f_T \equiv \partial f(R,T)/\partial T$.

The covariant derivative of Equation (3.2) yields

$$\nabla^\mu T_{\mu\nu} = \frac{f_T}{8\pi + f_T} \times \left[(L_m g_{\mu\nu} - T_{\mu\nu})\nabla^\mu \ln f_T + \nabla^\mu\left(L_m - \frac{1}{2}T\right)g_{\mu\nu}\right]. \tag{3.3}$$

As seen, the energy-momentum tensor is not conserved in the $f(R,T)$ theory. (For discussions on the violation of the conservation law of the energy momentum tensor, see the references [49, 57]). In this study, the matter forming the wormholes is assumed to be described by an anisotropic energy-momentum tensor

$$T_{\mu\nu} = -p_t(r)g_{\mu\nu} + (p_t(r) + \rho(r))U_\mu U_\nu + (p_r(r) - p_t(r))N_\mu N_\nu, \tag{3.4}$$

where $\rho(r)$, $p_r(r)$, and $p_t(r)$ are the energy density, the radial pressure, and the tangential pressure of the fluid, respectively, and the matter Lagrangian is assumed to be defined as $L_m = \frac{1}{3}(p_r + 2p_t)$. the four velocity U^μ and the radial unit vector N^μ satisfy the conditions $U_\nu U^\nu = 1$, $N_\nu N^\nu = -1$ and $U_\nu N^\nu = 0$.

3.1. Field equations for the case $R - a_1^2/R + a_2 T$

For the first case, by substituting the $R - a_1^2/R + a_2 T$ in Equation (3.2) yields

$$R_{\mu\nu}\left(1+\frac{a_1^2}{R^2}\right)+\frac{1}{2}Rg_{\mu\nu}(\frac{a_1^2}{R^2}-1)=(8\pi+a_2)T_{\mu\nu}+a_2 g_{\mu\nu}\left(\frac{1}{2}T-L_m\right)+a_1^2(\nabla_\mu\nabla_\nu-g_{\mu\nu}\nabla^\mu\nabla_\nu)(R^{-2}) \quad (3.5)$$

Moreover, by substituting the above form for $f(R,T)$ in Equation 3.3 yields (the same result also applies to the second case 3.2),

$$\nabla^\mu T_{\mu\nu}=\frac{a_2}{8\pi+a_2}\left(\nabla_\nu\left(L_m-\frac{1}{2}T\right)\right). \quad (3.6)$$

As seen in Equation (3.6), when $a_2 \to 0$, the conservation condition is satisfied.

The values of $r_0=1, \delta_0=1, \alpha=1, M=1$ were used in solving the field equations determined by Equation (3.5), and sets of equations were obtained for $\beta=1, \beta=2, \beta=3$. From these sets of equations, density and pressure values were obtained separately.

The expressions for density and pressure for $\beta=1$ have been obtained as follows:

$$\begin{aligned}\rho=-&\frac{1}{24(a_2+4\pi)(a_2+8\pi)r^6\left(-5r^2+2r+1\right)^4}\times\\&(96\pi r^2(1+8r+4r^2-88r^3-74r^4+440r^5+\\&100r^6-1000r^7+625r^8+2a_1^2r^{10}+12a_1^2r^{11}-\\&578a_1^2r^{12}-1992a_1^2r^{13}+2710a_1^2r^{14}+\\&8620a_1^2r^{15}-8870a_1^2r^{16}-7040a_1^2r^{17}+7200a_1^2r^{18})+\\&a_2(1+10r+35r^2+40r^3-190r^4-1028r^5-130r^6+\\&5800r^7+125r^8-13750r^9+9375r^{10}+28a_1^2r^{12}+\\&24a_1^2r^{13}-8596a_1^2r^{14}-26928a_1^2r^{15}+\\&40484a_1^2r^{16}+117080a_1^2r^{17}-125740a_1^2r^{18}-\\&96160a_1^2r^{19}+100800a_1^2r^{20}))\end{aligned} \quad (3.7)$$

$$\begin{aligned}p_r=&\frac{1}{24(a_2+4\pi)(a_2+8\pi)r^6\left(-5r^2+2r+1\right)^4}\times\\&(96\pi r(-1-2r+5r^2)(-1-5r+10r^2+55r^3-70r^4-\\&187r^5+290r^6+25r^7-125r^8-2a_1^2r^{11}-\\&36a_1^2r^{12}+64a_1^2r^{13}+336a_1^2r^{14}-438a_1^2r^{15}-\\&260a_1^2r^{16}+320a_1^2r^{17})+\\&a_2(1+34r+179r^2-272r^3-2686r^4+1324r^5+\\&16094r^6-11144r^7-39235r^8+46850r^9+3375r^{10}-\\&15000r^{11}+28a_1^2r^{12}+696a_1^2r^{13}+5228a_1^2r^{14}+\end{aligned}$$

$$5424a_1^2r^{15} - 22492a_1^2r^{16} - 22216a_1^2r^{17} + 39380a_1^2r^{18} + 26240a_1^2r^{19} - 33600a_1^2r^{20})) \tag{3.8}$$

$$p_t = \frac{1}{24(a_2+4\pi)(a_2+8\pi)r^6\left(-5r^2+2r+1\right)^4} \times (24\pi(-1-12r-31r^2+114r^3+462r^4-576r^5-2406r^6+2652r^7+4755r^8-7300r^9+1125r^{10}+1250r^{11}+4a1^2r^{12}+112a_1^2r^{13}-1804a_1^2r^{14}-7640a_1^2r^{15}+8124a_1^2r^{16}+32448a_1^2r^{17}-29940a_1^2r^{18}-26680a_1^2r^{19}+25600a_1^2r^{20})+a_2(-5-62r-175r^2+532r^3+2486r^4-2372r^5-12790r^6+11152r^7+26255r^8-33550r^9+1125r^{10}+7500r^{11}+4a_1^2r^{12}+408a_1^2r^{13}-5548a_1^2r^{14}-24960a_1^2r^{15}+24188a_1^2r^{16}+104888a_1^2r^{17}-92500a_1^2r^{18}-87280a_1^2r^{19}+81600a_1^2r^{20})) \tag{3.9}$$

The expressions for density and pressure for $\beta = 2$ and $\beta = 3$ have been obtained as follows:

$$\rho = -\frac{1}{24(a_2+4\pi)(a_2+8\pi)r^7\left(-1-3r+8r^2+r^3\right)^4} \times (192\pi r^2(1+12r+22r^2-184r^3-435r^4+1428r^5+1882r^6-6012r^7+1750r^8+1756r^9+372r^{10}+32r^{11}+(1+a_1^2)r^{12}+9a_1^2r^{13}-371a_1^2r^{14}-2022a_1^2r^{15}+1606a_1^2r^{16}+12103a_1^2r^{17}-9089a_1^2r^{18}-4431a_1^2r^{19}-13076a_1^2r^{20}+12855a_1^2r^{21}+2816a_1^2r^{22}+144a_1^2r^{23})+a_2(1+15r+90r^2+265r^3-295r^4-5787r^5-7570r^6+45765r^7+42510r^8-187260r^9+67652r^{10}+55590r^{11}+10245r^{12}+655r^{13}+28a_1^2r^{14}+(-1+84a_1^2)r^{15}-11276a_1^2r^{16}-55320a_1^2r^{17}+51400a_1^2r^{18}+330460a_1^2r^{19}-254444a_1^2r^{20}-129996a_1^2r^{21}-359120a_1^2r^{22}+361668a_1^2r^{23}+78944a_1^2r^{24}+4032a_1^2r^{25})) \tag{3.10}$$

$$p_r = \frac{1}{24(a_2+4\pi)(a_2+8\pi)r^6\left(-5r^2+2r+1\right)^4} \times (96\pi r(-1-3r+8r^2+r^3)(-1-8r+6r^2+124r^3-69r^4-636r^5+842r^6-224r^7+438r^8-388r^9-$$

$$184r^{10} - 24r^{11} - r^{12} - 2a_1^2r^{13} - 44a_1^2r^{14} +$$
$$46a_1^2r^{15} + 592a_1^2r^{16} - 736a_1^2r^{17} - 128a_1^2r^{18} -$$
$$482a_1^2r^{19} + 620a_1^2r^{20} + 64a_1^2r^{21}) -$$
$$a_2(-1 - 39r - 306r^2 + 71r^3 + 6319r^4 + 3267r^5 -$$
$$57494r^6 + 7467r^7 + 226842r^8 - 253332r^9 + 61372r^{10} -$$
$$82374r^{11} + 57771r^{12} + 43769r^{13} + (9000 - 28a_1^2)r^{14} +$$
$$(769 - 852a_1^2)r^{15} + (24 - 8212a_1^2)r^{16} - 15720a_1^2r^{17} +$$
$$42872a_1^2r^{18} + 79652a_1^2r^{19} - 75508a_1^2r^{20} -$$
$$60276a_1^2r^{21} - 126736a_1^2r^{22} + 152508a_1^2r^{23} +$$
$$29056a_1^2r^{24} + 1344a_1^2r^{25})) \tag{3.11}$$

$$p_t = \frac{1}{24(a_2 + 4\pi)(a_2 + 8\pi)r^6\left(-5r^2 + 2r + 1\right)^4} \times$$
$$(24\pi(-1 - 17r - 76r^2 + 147r^3 + 1501r^4 - 311r^5 -$$
$$11772r^6 + 4367r^7 + 40160r^8 - 41840r^9 - 900r^{10} -$$
$$1630r^{11} + 7327r^{12} + 4071r^{13} + (782 + 4a_1^2)r^{14} +$$
$$5(13 + 28a_1^2)r^{15} + (2 - 2220a_1^2)r^{16} - 15304a_1^2r^{17} +$$
$$7848a_1^2r^{18} + 91012a_1^2r^{19} - 63900a_1^2r^{20} -$$
$$27652a_1^2r^{21} - 99800a_1^2r^{22} + 92540a_1^2r^{23} +$$
$$20168a_1^2r^{24} + 1024a1^2r^{25}) +$$
$$a_2(-5 - 87r - 414r^2 + 571r^3 + 7655r^4 + 1179r^5 -$$
$$57322r^6 + 3423r^7 + 193134r^8 - 149724r^9 - 21748r^{10} -$$
$$38478r^{11} + 36351r^{12} + 23545r^{13} +$$
$$4(1161 + a_1^2)r^{14} + (389 + 492a_1^2)r^{15} +$$
$$(12 - 6788a_1^2)r^{16} - 50088a_1^2r^{17} + 21400a_1^2r^{18} +$$
$$295588a_1^2r^{19} - 201572a_1^2r^{20} - 83220a_1^2r^{21} -$$
$$330272a_1^2r^{22} + 299868a_1^2r^{23} + 64784a_1^2r^{24} + 3264a_1^2r^{25})) \tag{3.12}$$

$$\rho = -\frac{1}{24(a_2 + 4\pi)(a_2 + 8\pi)r^8\left(-1 - 4r + 12r^2 + r^4\right)^4} \times$$
$$((96\pi r^2(3 + 48r + 144r^2 - 960r^3 - 3564r^4 + 11376r^5 +$$
$$20592r^6 - 80256r^7 + 63954r^8 - 20592r^9 + 20592r^{10} -$$
$$1728r^{11} + 2580r^{12} - 48r^{13} + 2(72 + a_1^2)r^{14} +$$
$$24a_1^2r^{15} + (3 - 924a_1^2)r^{16} - 7008a_1^2r^{17} +$$
$$4666a_1^2r^{18} + 61392a_1^2r^{19} - 75848a_1^2r^{20} +$$

$$11040a_1^2r^{21} - 14394a_1^2r^{22} - 69096a_1^2r^{23} + 88580a_1^2r^{24} - 3648a_1^2r^{25} + 9790a_1^2r^{26} + 288a_1^2r^{28}) + a_2(1 + 20r + 160r^2 + 640r^3 - 165r^4 - 16336r^5 - 35040r^6 + 183040r^7 + 244970r^8 - 1209480r^9 + 995808r^{10} - 275840r^{11} + 306710r^{12} - 17360r^{13} + 34400r^{14} + (1445 + 28a_1^2)r^{16} + 4(5 + 36a_1^2)r^{17} - 14304a_1^2r^{18} - 96192a_1^2r^{19} + (-1 + 79724a_1^2)r^{20} + 832320a_1^2r^{21} - 1049152a_1^2r^{22} + 149760a_1^2r^{23} - 214764a_1^2r^{24} - 946992a_1^2r^{25} + 1239136a_1^2r^{26} - 48192a_1^2r^{27} + 137060a_1^2 2r^{28} + 96a_1^2r^{29} + 4032a_1^2r^{30})) \quad (3.13)$$

$$p_r = \frac{1}{24(a_2 + 4\pi)(a_2 + 8\pi)r^8\left(-1 - 4r + 12r^2 + r^4\right)^4} \times (96\pi r(-1 - 4r + 12r^2 + r^4)(-1 - 11r + 236r^3 - 76r^4 - 1839r^5 + 3420r^6 - 2216r^7 + 570r^8 + 1263r^9 - 1656r^{10} + 252r^{11} - 428r^{12} + 11r^{13} - 36r^{14} - 2a_1^2r^{15} - (1 + 52a_1^2)r^{16} + 20a_1^2r^{17} + 992a_1^2r^{18} - 1484a_1^2r^{19} + 72a_1^2r^{20} - 116a_1^2r^{21} - 784a_1^2r^{22} + 1150a_1^2r^{23} - 20a_1^2r^{24} + 64a_1^2r^{25}) + a_2(1 + 44r + 448r^2 + 256r^3 - 12453r^4 - 14152r^5 + 169632r^6 - 17408r^7 - 1048342r^8 + 1898856r^9 - 1306464r^{10} + 383104r^{11} + 275990r^{12} - 453056r^{13} + 116192r^{14} - 162048r^{15} + 7(1523 + 4a_1^2)r^{16} + 4(-5149 + 252a_1^2)r^{17} + 288(1 + 41a_1^2)r^{18} + 192(-6 + 163a_1^2)r^{19} - (1 + 86164a_1^2)r^{20} - 24(1 + 8996a_1^2)r^{21} + 340160a_1^2r^{22} - 40704a_1^2r^{23} + 109332a_1^2r^{24} + 377328a_1^2r^{25} - 557984a_1^2r^{26} + 8640a_1^2r^{27} - 51868a_1^2r^{28} - 384a_1^2r^{29} - 1344a_1^2r^{30})) \quad (3.14)$$

$$p_t = \frac{1}{24(a_2 + 4\pi)(a_2 + 8\pi)r^8\left(-1 - 4r + 12r^2 + r^4\right)^4} \times (24\pi(-1 - 22r - 136r^2 + 160r^3 + 3493r^4 + 794r^5 - 39040r^6 + 15680r^7 + 192278r^8 - 333644r^9 + 219312r^{10} - 108544r^{11} + 25322r^{12} + 26020r^{13} + 64r^{14} + 12736r^{15} + (91 + 4a_1^2)r^{16} + 6(283 + 28a_1^2)r^{17} -$$

$$8(-3+332a_1^2)r^{18}-32(-3+830a_1^2)r^{19}+(1+8756a_1^2)r^{20}+$$
$$(2+237304a_1^2)r^{21}-280192a_1^2r^{22}+42752a_1^2r^{23}-$$
$$42548a_1^2r^{24}-268904a_1^2r^{25}+327904a_1^2r^{26}-$$
$$14912a_1^2r^{27}+35324a_1^2r^{28}-56a_1^2r^{29}+1024a_1^2r^{30})+$$
$$a_{-2}(-5-112r-728r^2+448r^3+17337r^4+11468r^5-$$
$$183744r^6+4096r^7+904430r^8-1285200r^9+776784r^{10}-$$
$$432896r^{11}-35566r^{12}+180232r^{13}-27136r^{14}+$$
$$77568r^{15}+(-1465+4a_1^2)r^{16}+$$
$$32(319+18a_1^2)r^{17}+(72-8064a_1^2)r^{18}-$$
$$192(-3+455a_1^2)r^{19}+(5+20276a_1^2)r^{20}+$$
$$12(1+65228a_1^2)r^{21}-909952a_1^2r^{22}+141312a_1^2r^{23}-$$
$$124596a_1^2r^{24}-902112a_1^2r^{25}+1080640a_1^2r^{26}-$$
$$50112a_1^2r^{27}+114044a_1^2r^{28}-240a_1^2r^{29}+3264a_1^2r^{30})) \tag{3.15}$$

3.2. Field equations for the case $R+a_1^2R^2+a_2T$

For the second case, by substituting the $R+a_1^2R^2+a_2T$ in Equation (3.2) yields

$$R_{\mu\nu}\left(1+2a_1^2R^2\right)-\frac{1}{2}Rg_{\mu\nu}(a_1^2R+1)=$$
$$(8\pi+a_2)T_{\mu\nu}+a_2g_{\mu\nu}\left(\frac{1}{2}T-L_m\right)+$$
$$2a_1^2(\nabla_\mu\nabla_\nu-g_{\mu\nu}\nabla^\mu\nabla_\nu)R \tag{3.16}$$

The values of $r_0=1,\delta_0=1,\alpha=1,M=1$ were used in solving the field equations determined by Equation (3.16), and sets of equations were obtained for $\beta=1,\beta=2,\beta=3$. From these sets of equations, density and pressure values were obtained separately.

The expressions for density and pressure for $\beta=1$ have been obtained as follows:

$$\rho=-\frac{1}{48(a_2+4\pi)(a_2+8\pi)r^{12}}\times$$
$$(-2r^6(a_2+2a_2r+15a_2r^2+96\pi r^2)+$$
$$a_1^2(24\pi(-1-4r+286r^2+404r^3-865r^4-320r^5+480r^6)+$$
$$a_2(-5-56r+938r^2+1576r^3-2945r^4-1240r^5+1680r^6))) \tag{3.17}$$

$$p_r=-\frac{1}{48(a_2+4\pi)(a_2+8\pi)r^{12}}\times$$
$$(-2r^6(96\pi r(-1+r+r^2)+a_2(-1-26r+33r^2+24r^3))+$$

$$a_1^2(24\pi(1-12r+58r^2+180r^3-327r^4-200r^5+320r^6)+ \\ a_2(5-40r+1126r^2+1928r^3-4207r^4-1880r^5+3120r^6))) \tag{3.18}$$

$$p_t=\frac{1}{48(a_2+4\pi)(a_2+8\pi)r^{12}}\times \\ (2r^6(24\pi(-1-4r+5r^2+2r^3)+ \\ a_2(-5-22r+21r^2+12r^3))- \\ a_1^2(24\pi(1+32r+378r^2+332r^3- \\ 1111r^4-300r^5+640r^6)+ \\ a_2(7+160r+1490r^2+1144r^3- \\ 4421r^4-1120r^5+2640r^6))) \tag{3.19}$$

The expressions for density and pressure for $\beta=2$ have been obtained as follows:

$$\rho=\frac{1}{48(a_2+4\pi)(a_2+8\pi)r^{14}}\times \\ (-384\pi r^9+2a_2r^7(-1-3r-32r^2+r^3)+ \\ a_1^2(24\pi(-1-6r+411r^2+938r^3-1690r^4-480r^5- \\ 721r^6+1280r^7+96r^8)+ \\ a_2(-5-72r+1317r^2+3526r^3-5744r^4-1572r^5- \\ 2765r^6+4456r^7+336r^8))) \tag{3.20}$$

$$p_r=\frac{1}{48(a_2+4\pi)(a_2+8\pi)r^{14}}\times \\ (-2r^7(96\pi r(-1+r+r^3)+ \\ a_2(-1-27r+40r^2+r^3+24r^4))+ \\ a_1^2(24\pi(1-14r+49r^2+310r^3-490r^4 \\ -104r^5-383r^6+632r^7+64r^8)+ \\ a_2(5-48r+1443r^2+3962r^3-7336r^4-1932r^5- \\ 3859r^6+7016r^7+624r^8))) \tag{3.21}$$

$$p_t=\frac{1}{48(a_2+4\pi)(a_2+8\pi)r^{14}}\times \\ (2r^7(24\pi(-1-5r+6r^2+r^3+2r^4)+ \\ a_2(-5-27r+20r^2+5r^3+12r^4))- \\ a_1^2(24\pi(1+38r+557r^2+850r^3-2106r^4-640r^5- \\ 671r^6+1620r^7+128r^8)+$$

$$a_2(7+192r+2193r^2+2998r^3-8240r^4-2532r^5- \\ 2465r^6+6496r^7+528r^8))) \tag{3.22}$$

The expressions for density and pressure for $\beta=3$ have been obtained as follows:

$$\rho=\frac{1}{48(a_2+4\pi)(a_2+8\pi)r^{16}}\times \\ (-384\pi r^9+2a_2r^7(-1-3r-32r^2+r^3)+ \\ (2r^8(-288\pi r^2+a_2(-1-4r-48r^2+r^4))+ \\ a_1^2(24\pi(-1-8r+560r^2+1792r^3-3886r^4+8r^5- \\ 608r^6-1344r^7+2879r^8+96r^{10})+ \\ a_2(-5-88r+1768r^2+6704r^3-13382r^4+112r^5- \\ 1960r^6-5136r^7+10075r^8-24r^9+336r^{10}))) \tag{3.23}$$

$$p_r=\frac{1}{48(a_2+4\pi)(a_2+8\pi)r^{16}}\times \\ (-2r^8(96\pi r(-1+r+r^4)+ \\ a_2(-1-28r+48r^2+r^4+24r^5))+ \\ a_1^2(24\pi(1-16r+32r^2+512r^3-914r^4+24r^5- \\ 80r^6-640r^7+1153r^8-8r^9+64r^{10})+ \\ a_2(5-56r+1784r^2+7120r^3-15418r^4+80r^5- \\ 2168r^6-6768r^7+14117r^8-24r^9+624r^{10}))) \tag{3.24}$$

$$p_t=\frac{1}{48(a_2+4\pi)(a_2+8\pi)r^{16}}\times \\ (2r^8(24\pi(-1-6r+8r^2+r^4+2r^5)+ \\ a_2(-5-32r+24r^2+5r^4+12r^5))- \\ a_1^2(24\pi(1+44r+768r^2+1616r^3-4562r^4-64r^5- \\ 816r^6-1232r^7+3457r^8+20r^9+128r^{10})+ \\ a_2(7+224r+3016r^2+5648r^3-17438r^4-320r^5- \\ 3208r^6-4464r^7+13543r^8+96r^9+528r^{10}))) \tag{3.25}$$

4. Energy and stability conditions

As discussed in detail in Section 1, in most cases, exotic matter that violates energy conditions is needed for wormholes to be stable and traversable. However, the existence of exotic matter is undesirable due to its physical properties. Therefore, whether traversable wormholes violate energy conditions is

of significant theoretical importance. Energy conditions are derived from the Raychaudhuri equation, which is not directly related to any specific theory of gravity. However, they have been studied within the framework of various gravitational theories, [58–61, 74, 75].

The wormholes with anisotropic matter distribution, the energy conditions are given as follows [76]:

1. Null Energy Condition: $\rho + p_r \geq 0, \rho + p_t \geq 0$,

2. Weak Energy Condition: $\rho \geq 0, \rho + p_r \geq 0, \rho + p_t \geq 0$,

3. Dominant Energy Condition: $\rho \geq 0, \rho \pm p_r \geq 0$, $\rho \pm p_t \geq 0$,

4. Strong Energy Condition: $\rho + p_r \geq 0, \rho + p_t \geq 0$, $\rho + p_r + 2p_t \geq 0$.

In this study, we also considered the stability conditions of the wormhole solutions for the model we chose using the generalized Tolman-Oppenheimer-Volkoff (TOV) equation:

$$\frac{dp_r}{dr} + \frac{\delta'(\rho + p_r)}{2} + \frac{2}{r}(p_r - p_t) = 0, \tag{4.1}$$

This equation allows us to examine the stability of the wormhole with the help of gravitational force, F_{gf}, anisotropic force, F_{af}, and hydrostatic force, F_{hf}. The gravitational force is a result of the wormhole's gravitational attraction, while the anisotropic force stems from the system's anisotropy, and finally, the hydrostatic force arises as a result of the hydrostatic fluid, which we assume forms the wormhole. For the wormhole to be in equilibrium, the condition $F_{gf} + F_{af} + F_{hf} = 0$ must be satisfied. In this study, the stability conditions for the cases $\beta = 1$, $\beta = 2$, and $\beta = 3$ were examined, and the other parameter values were chosen as $r_0 = 1$, $\delta_0 = 1$, $\alpha = 1$, and $M = 1$. In 4.1 and 4.2, where the energy and stability conditions are examined, the parameters a_1 and a_2 are chosen as 9π and -9π, respectively.

4.1. Energy and stability conditions for the case $R - a_1^2/R + a_2 T$

The evolution of the gravitational force, anisotropic force, and hydrostatic force for $\beta = 1$, $\beta = 2$, and $\beta = 3$ has been examined. However, the three beta values indicate that the geometry possesses an attractive feature (Figure 4). We can analyze this behavior using the dimensionless anisotropic parameter, $\Delta = \frac{p_t - p_r}{\rho}$, [77, 78]. In all three cases, since $\rho > 0$, if $p_t < p_r$, then $\Delta < 0$, which implies that the geometry is attractive. On the other hand, if $p_t > p_r$, the geometry is repulsive, and if $p_t = p_r$, the fluid is isotropic. The evolution of the energy and stability conditions in the case of $\beta = 1$ is presented in Figures 5 and 6, in the case of $\beta = 2$ is presented in Figures 7 and 8, and in the case of $\beta = 3$ is presented in Figures 9 and 10.

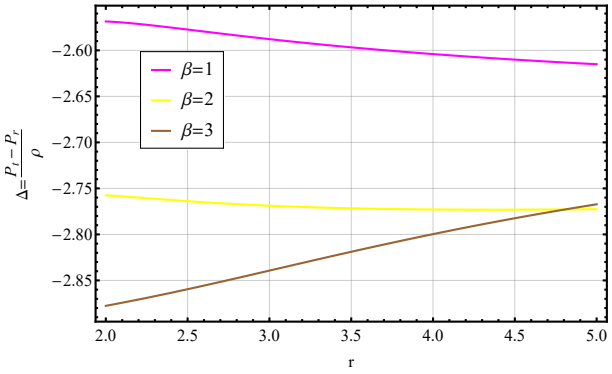


Figure 4. Signs of the anisotropy parameter for the case $R-a_1^2/R+a_2T$. The curves are plotted for different values of the β parameter, $\beta=1$, $\beta=2$, $\beta=3$ and the values $r_0=1, \delta_0=1, \alpha=1, M=1$ are chosen.

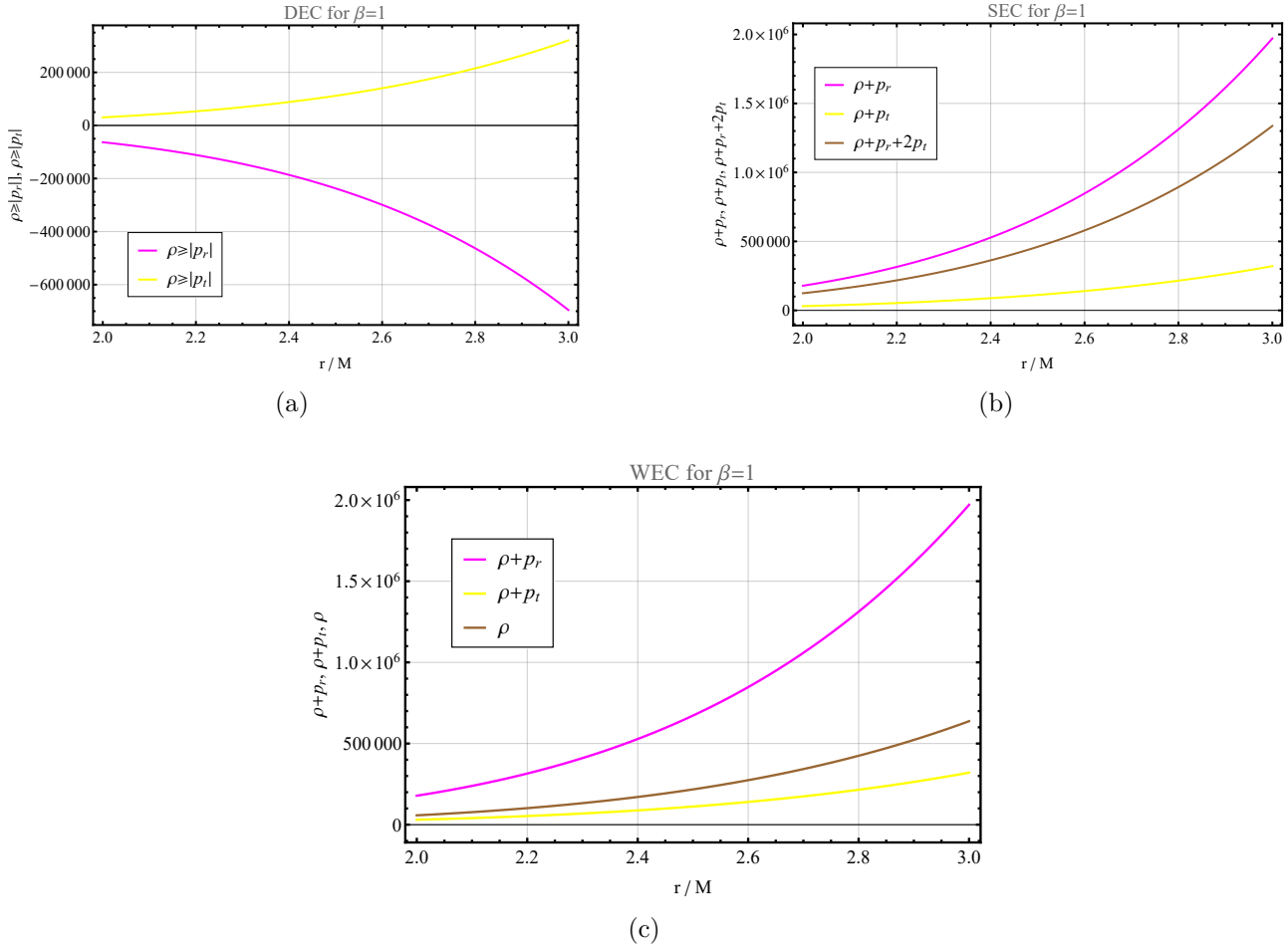


Figure 5. Behavior of energy conditions of the $R-a_1^2/R+a_2T$ case for $\beta=1$ and the values $r_0=1, \delta_0=1, \alpha=1, M=1$ are chosen.

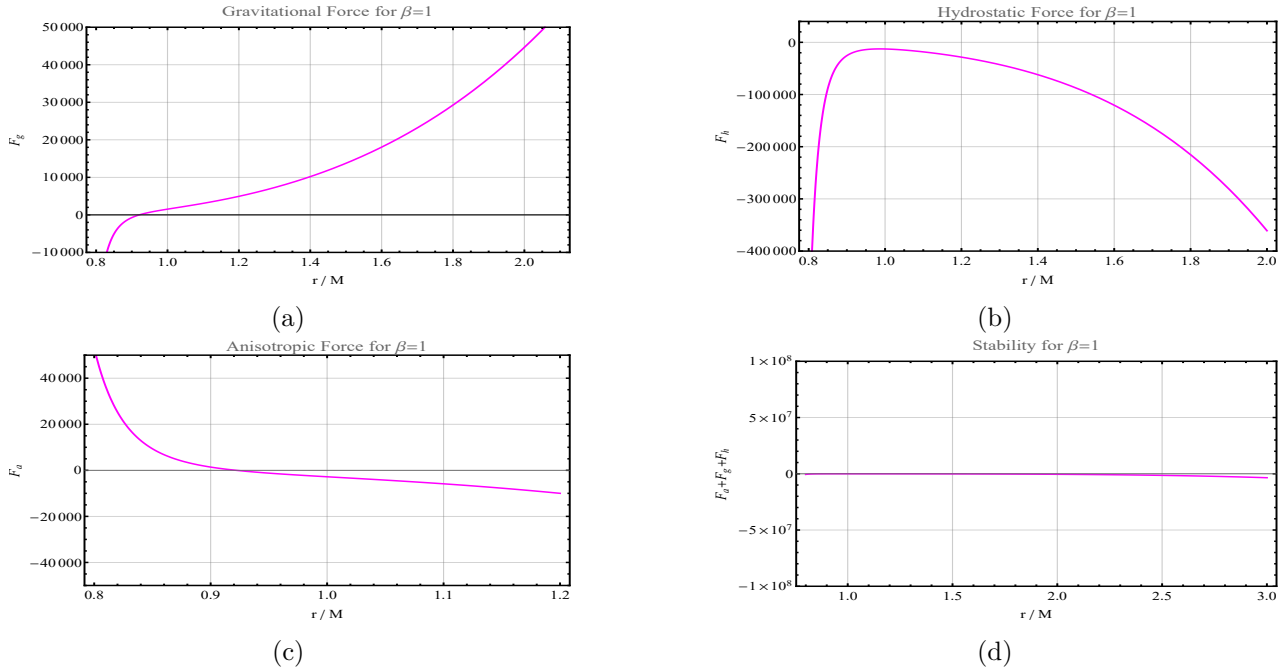


Figure 6. Stability of the $R - a_1^2/R + a_2 T$ case for $\beta = 1$ and the values $r_0 = 1,\ \delta_0 = 1,\ \alpha = 1,\ M = 1$ are chosen. F_g, F_a, and F_h represent gravitational force, anisotropic force, and hydrostatic force, respectively.

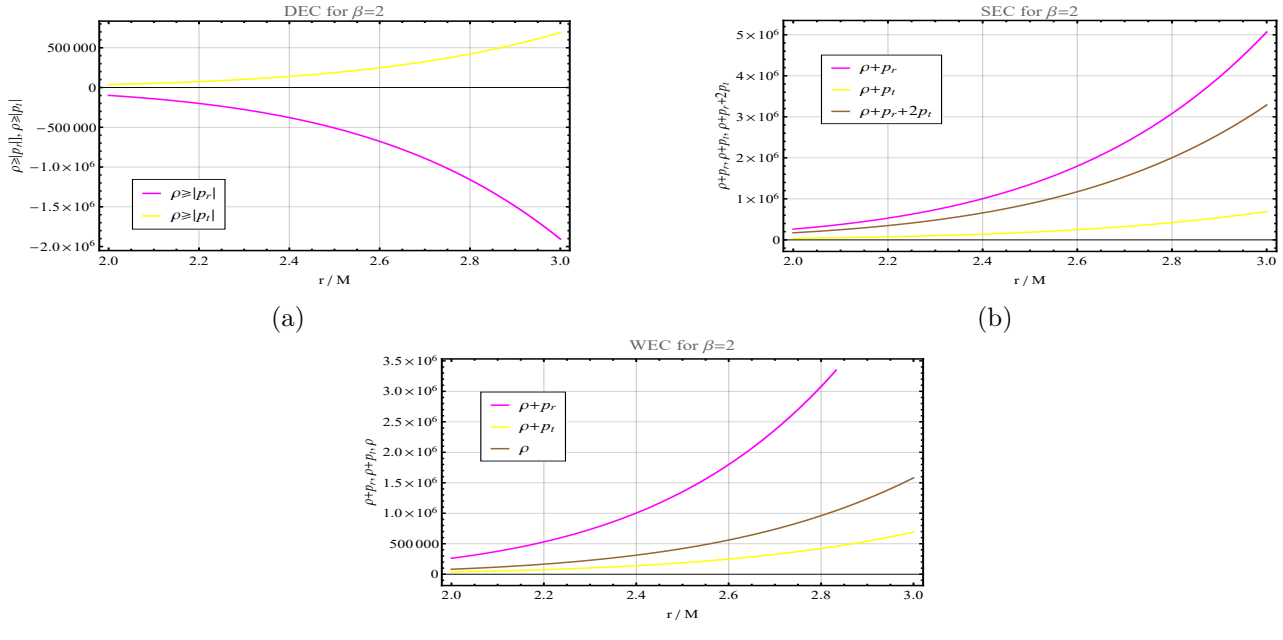


Figure 7. Behavior of energy conditions of the $R - a_1^2/R + a_2 T$ case for $\beta = 2$ and the values $r_0 = 1, \delta_0 = 1, \alpha = 1, M = 1$ are chosen.

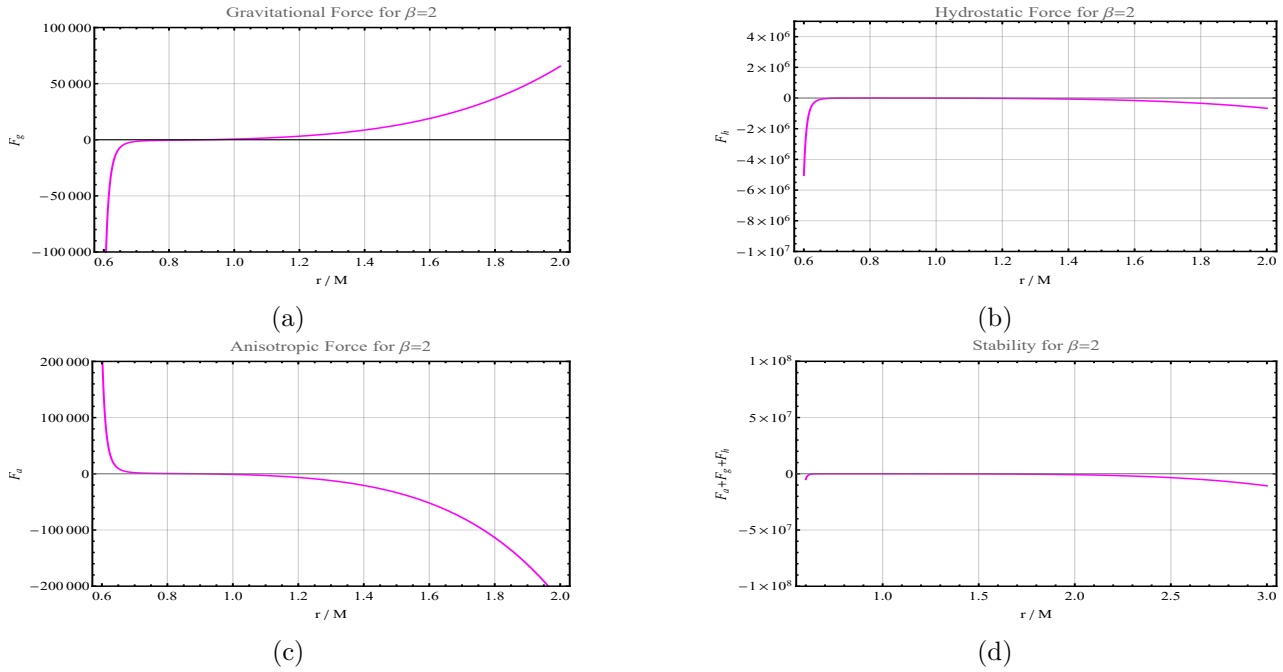


Figure 8. Stability of the $R - a_1^2/R + a_2 T$ case for $\beta = 2$ and the values $r_0 = 1$, $\delta_0 = 1$, $\alpha = 1$, $M = 1$ are chosen. F_g, F_a, and F_h represent gravitational force, anisotropic force, and hydrostatic force, respectively.

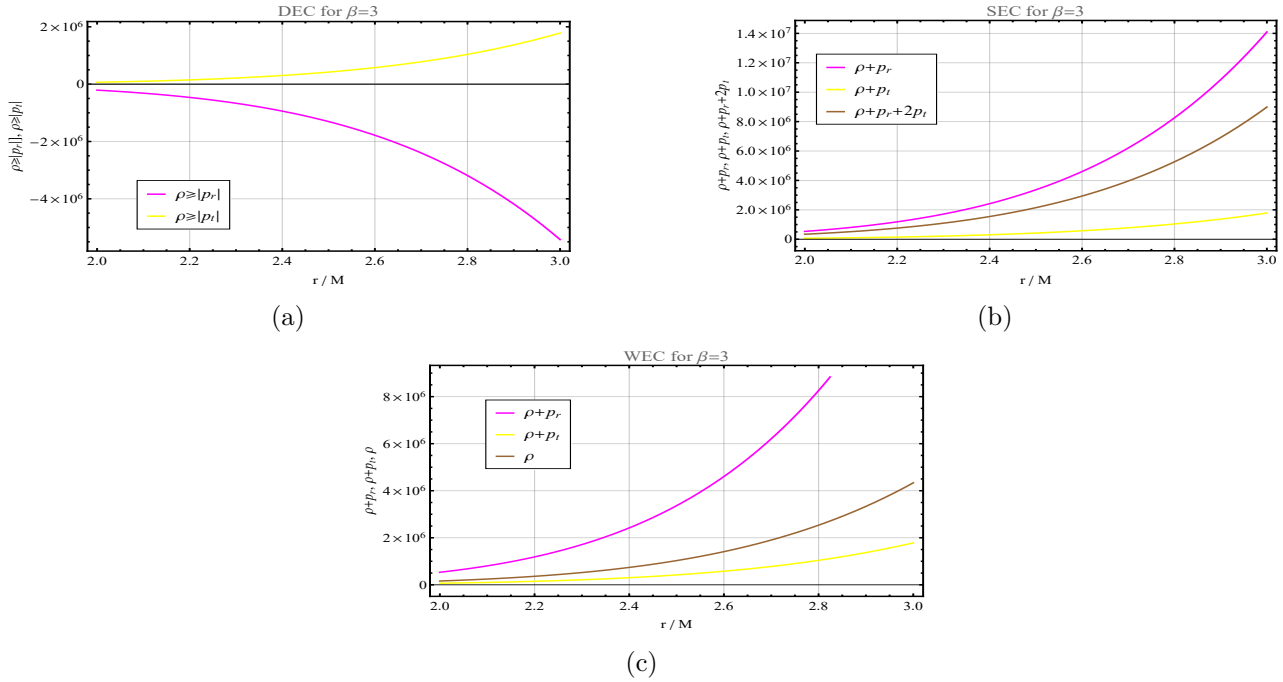


Figure 9. Behavior of energy conditions of the $R - a_1^2/R + a_2 T$ case for $\beta = 3$ and the values $r_0 = 1, \delta_0 = 1, \alpha = 1, M = 1$ are chosen.

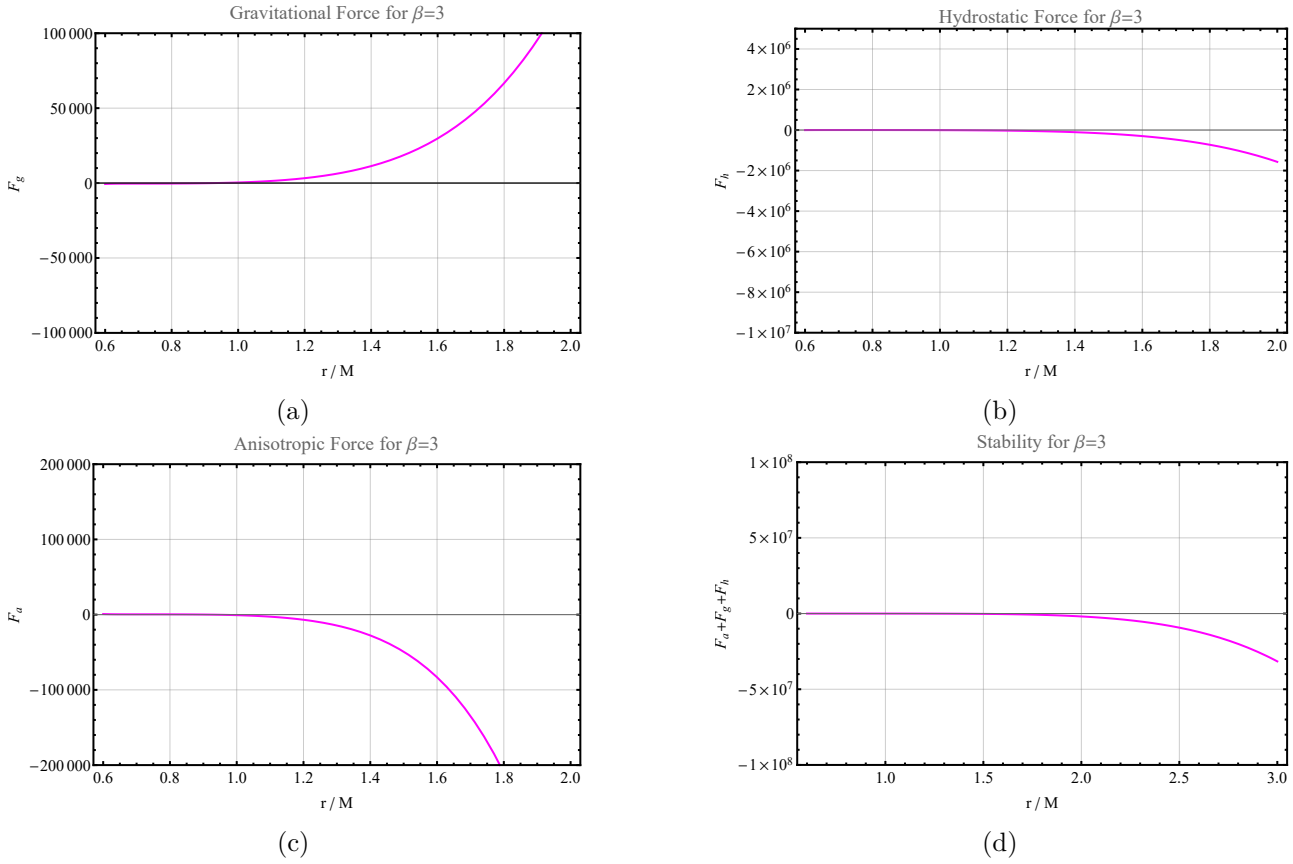


Figure 10. Stability of the $R - a_1^2/R + a_2T$ case for $\beta = 3$ and the values $r_0 = 1$, $\delta_0 = 1$, $\alpha = 1$, $M = 1$ are chosen. F_g, F_a, and F_h represent gravitational force, anisotropic force, and hydrostatic force, respectively.

4.2. Energy and stability conditions for the case $R + a_1^2R^2 + a_2T$

Just as in Section 4.1, the examination of the dimensionless anisotropic parameter demonstrates that gravity possesses an attractive character (Figure 11). The evolution of the energy and stability conditions in the case of $\beta = 1$ is presented in Figures 12 and 13, in the case of $\beta = 2$ is presented in Figures 14 and 15, and in the case of $\beta = 3$ is presented in Figures 16 and 17.

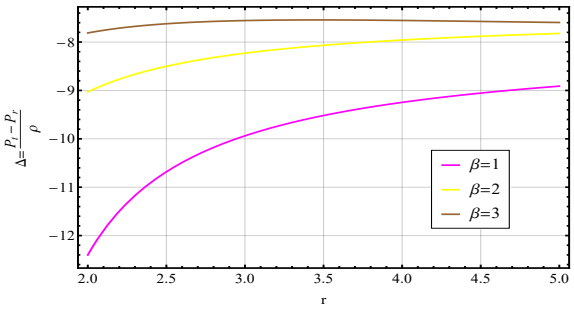


Figure 11. Signs of the anisotropy parameter for the case $R + a_1^2R^2 + a_2T$. The curves are plotted for different values of the β parameter, $\beta = 1$, $\beta = 2$, $\beta = 3$ and the values $r_0 = 1, \delta_0 = 1, \alpha = 1, M = 1$ are chosen.

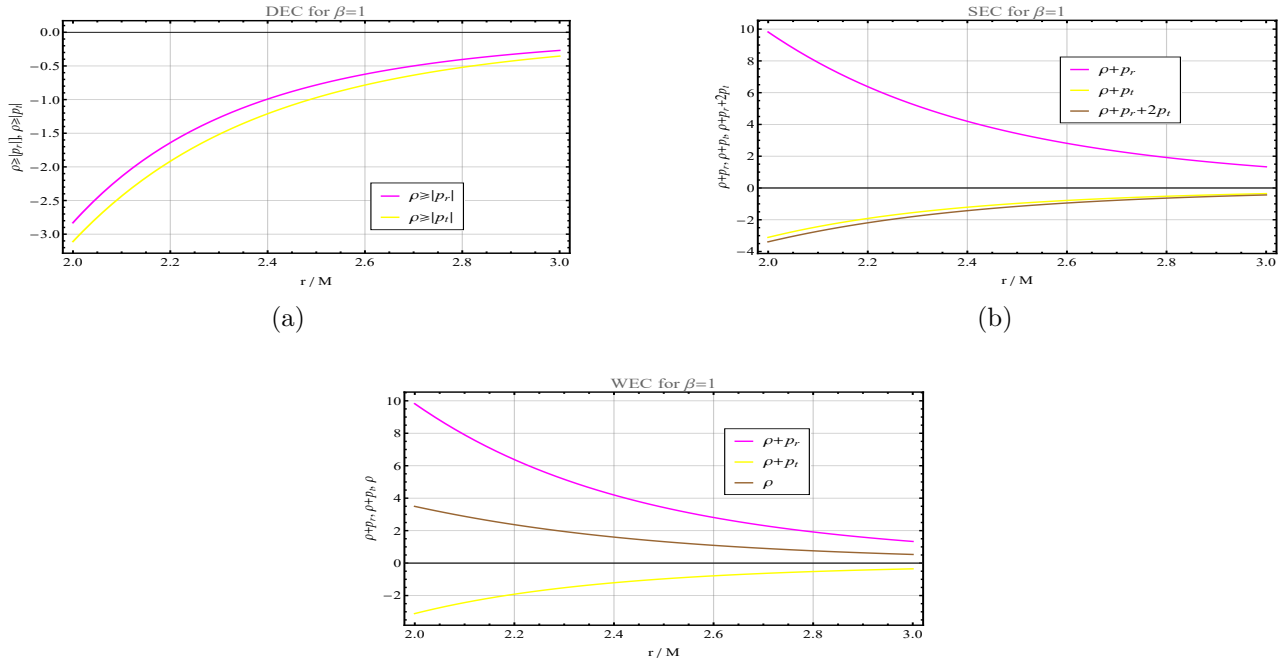


Figure 12. Behavior of energy conditions of the $R + a_1^2R^2 + a_2T$ case for $\beta = 1$ and the values $r_0 = 1$, $\delta_0 = 1$, $\alpha = 1$, $M = 1$ are chosen.

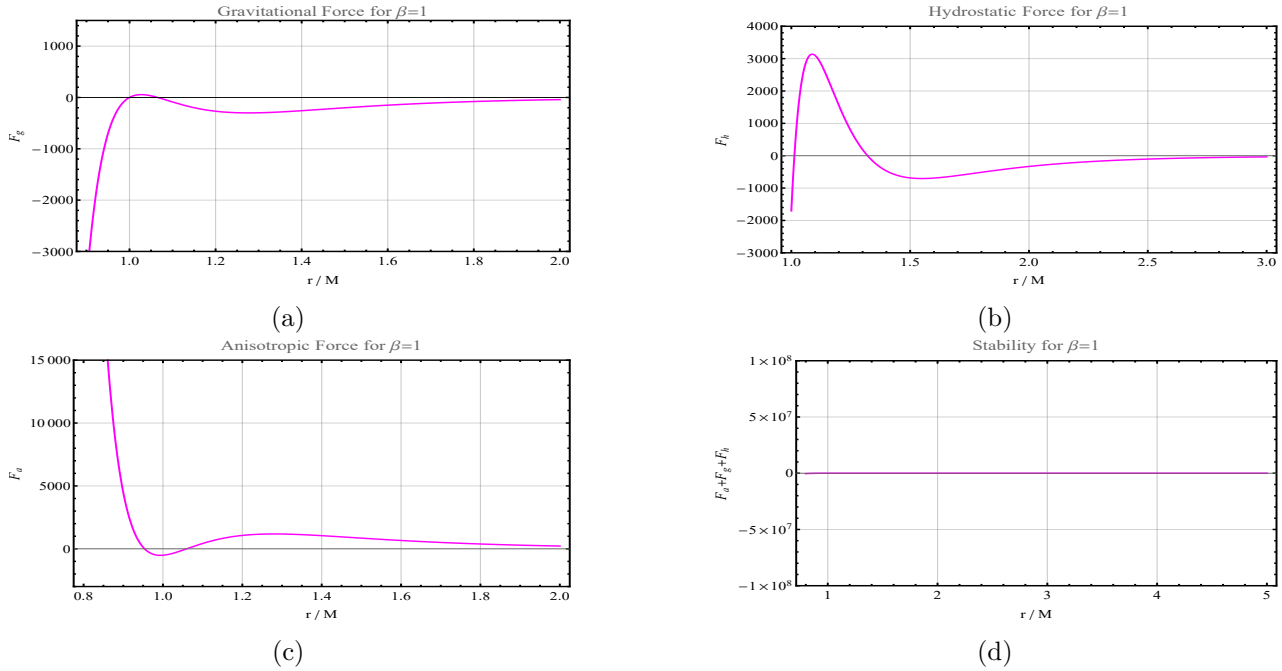


Figure 13. Stability of the $R + a_1^2R^2 + a_2T$ case for $\beta = 1$ and the values $r_0 = 1$, $\delta_0 = 1$, $\alpha = 1$, $M = 1$ are chosen. F_g, F_a, and F_h represent gravitational force, anisotropic force, and hydrostatic force, respectively.

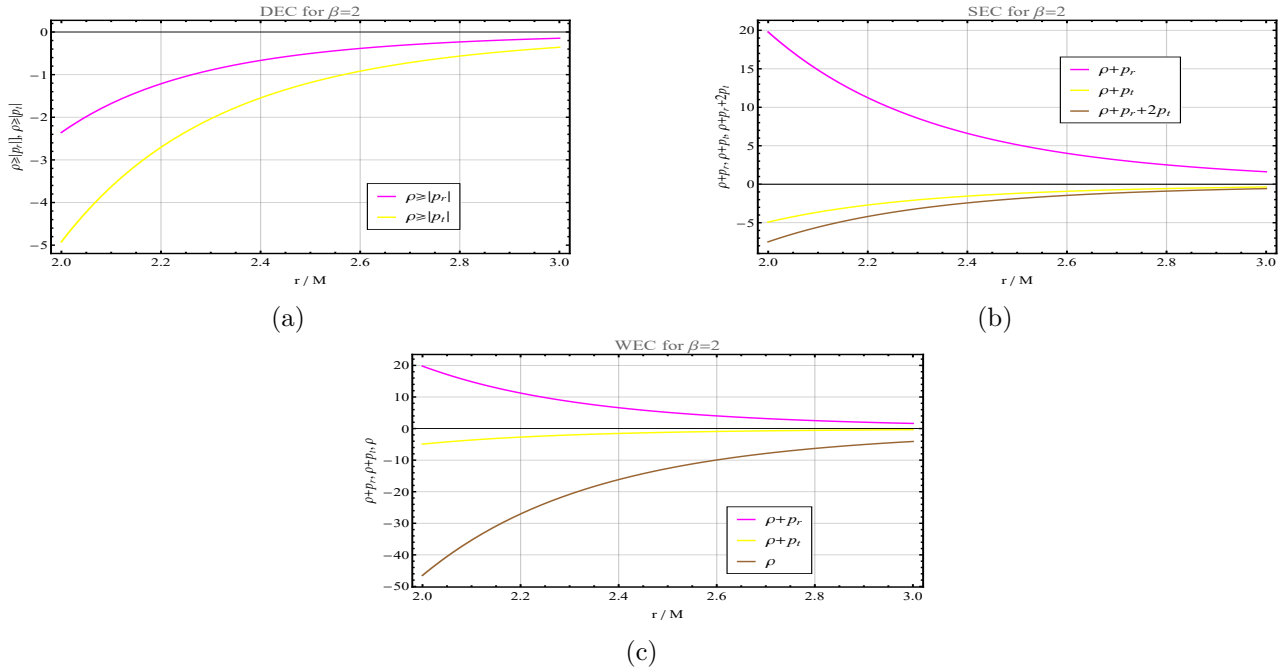


Figure 14. Behavior of energy conditions of the $R + a_1^2R^2 + a_2T$ case for $\beta = 2$ and the values $r_0 = 1$, $\delta_0 = 1$, $\alpha = 1$, $M = 1$ are chosen.

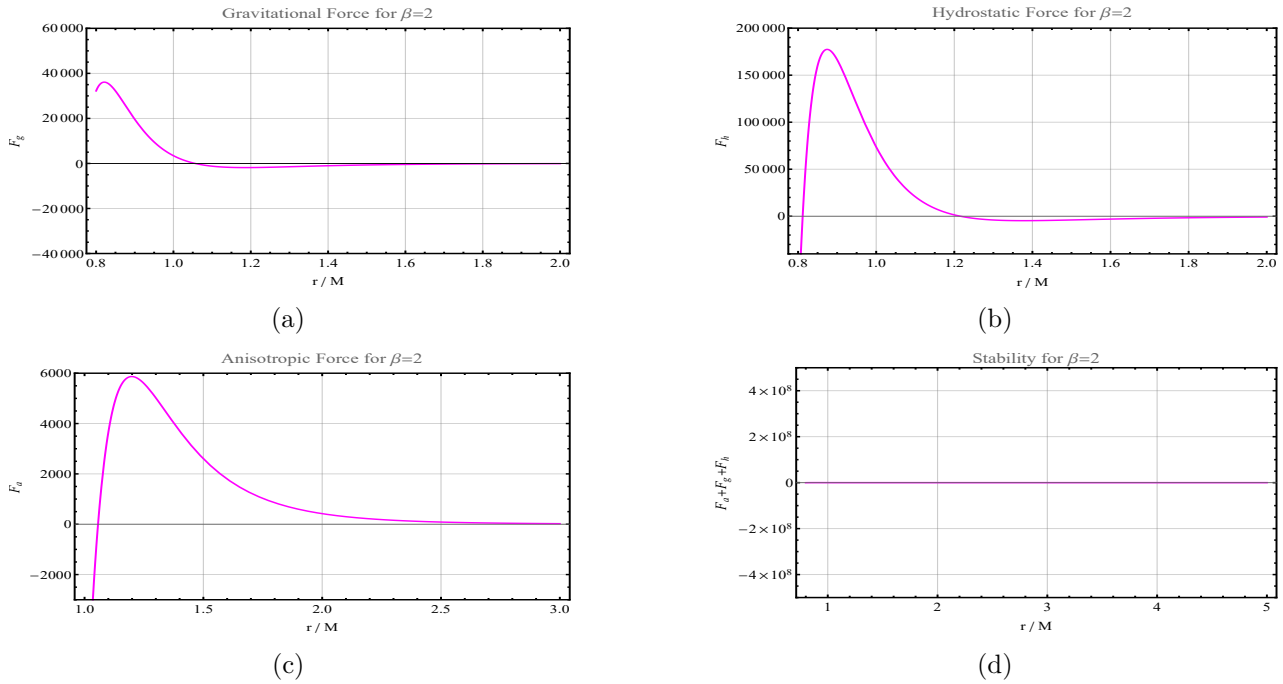


Figure 15. Stability of the $R + a_1^2R^2 + a_2T$ case for $\beta = 2$ and the values $r_0 = 1$, $\delta_0 = 1$, $\alpha = 1$, $M = 1$ are chosen. F_g, F_a, and F_h represent gravitational force, anisotropic force, and hydrostatic force, respectively.

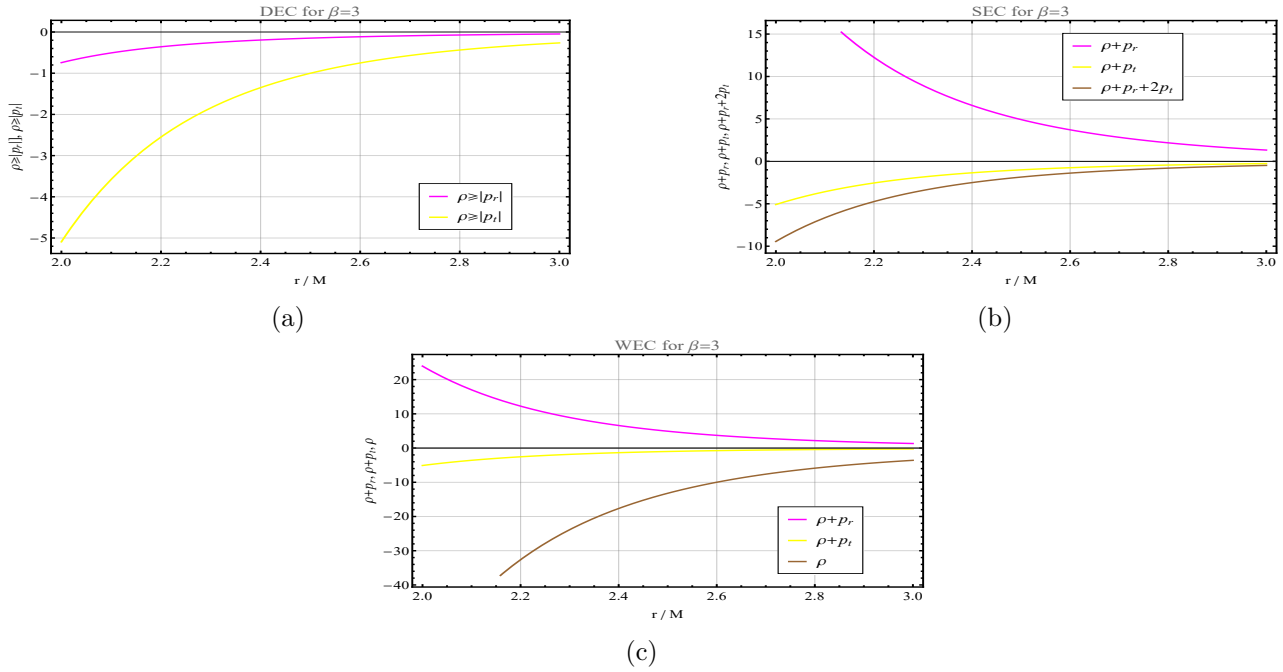


Figure 16. Behavior of energy conditions of the $R + a_1^2R^2 + a_2T$ case for $\beta = 3$ and the values $r_0 = 1$, $\delta_0 = 1$, $\alpha = 1$, $M = 1$ are chosen.

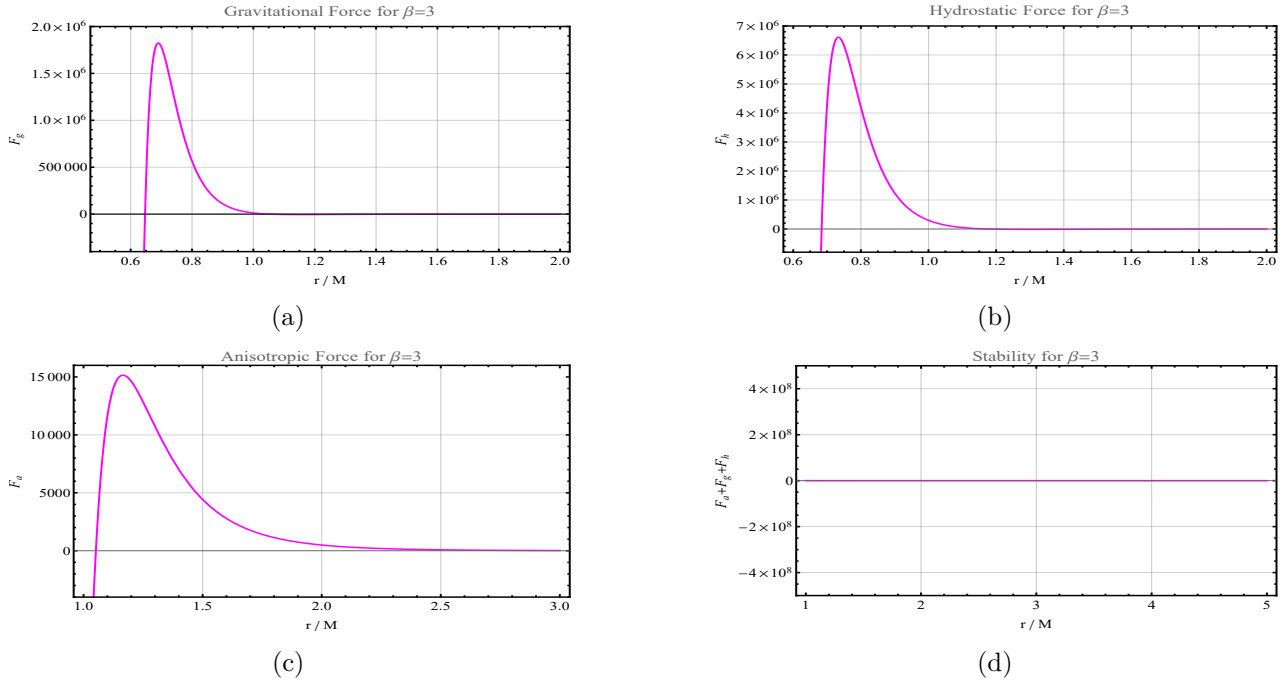


Figure 17. Stability of the $R + a_1^2R^2 + a_2T$ case for $\beta = 3$ and the values $r_0 = 1$, $\delta_0 = 1$, $\alpha = 1$, $M = 1$ are chosen. F_g, F_a, and F_h represent gravitational force, anisotropic force, and hydrostatic force, respectively.

5. Karmarkar condition

In this study, to understand the effect of the chosen redshift function on wormhole geometry, we examine the Karmarkar condition [79] and investigate whether the presence of exotic matter is necessary under the conditions we have established. In this context, static spherically symmetric spacetime can be written as;

$$ds^2 = -e^{\delta(r)}dt^2 + e^{\Sigma(r)}dr^2 + r^2d\theta^2 + r^2\sin^2\theta d\phi^2. \tag{5.1}$$

The nonzero components of the Riemann curvature according to the above space-time described by Equation 5.1 are given by:

$$R_{1414} = \frac{e^{\delta}(2\delta'' + \delta'^2 - \delta'\Sigma')}{4}, R_{1212} = \frac{r\Sigma'}{2}. \tag{5.2}$$

$$R_{2323} = \frac{r^2Sin^2\theta(e^{\Sigma} - 1)}{e^{\Sigma}}, R_{3434} = \frac{rSin^2\theta\Sigma'e^{\delta-\Sigma}}{2}. \tag{5.3}$$

Karmarkar condition is given as follows:

$$R_{1414} = \frac{R_{1212}R_{3434} + R_{1224}R_{1334}}{R_{2323}}, \tag{5.4}$$

with $R_{2323} \neq 0$. By substituting Riemann curvature in Karmarkar relation, we obtain:

$$\frac{\delta'\Sigma'}{1 - e^{\Sigma}} = \delta'\Sigma' - 2\delta'' - \delta'^2.$$

The solution of the above differential equation is given as

$$e^{\Sigma} = 1 + \Gamma e^{\delta}\delta'^2. \tag{5.5}$$

Here, Γ is an integrating constant. By comparing Equation 2.1 and Equation 5.1, we get

$$\Sigma(r) = Log[\frac{r}{r - b(r)}]. \tag{5.6}$$

Using Equations 5.5, 2.3, and 5.6, we find

$$b(r) = r - \frac{r}{1 + \Gamma e^{\delta}\delta'^2}. \tag{5.7}$$

As discussed in Section 2, when we apply the condition $b(r_0) - r_0 = 0$ to Equation 5.7, we arrive at the result $r_0 = 0$. To overcome this problem, we can add a constant C to Equation 5.7. Then, using the condition $b(r_0) - r_0 = 0$, we obtain the constant as $\Gamma = \frac{r_0^2(r_0 - C)}{e^{\delta}\alpha^2 b_0^2}$. After substituting the value of Γ into equation 5.7, we find

$$b(r) = r - \frac{r^{2\alpha+3}}{r^{2\alpha+2} + r_0^{2\alpha+2}(r_0 - C)}. \tag{5.8}$$

Using Eq. 5.8, we draw embedding diagrams (Figure 18).

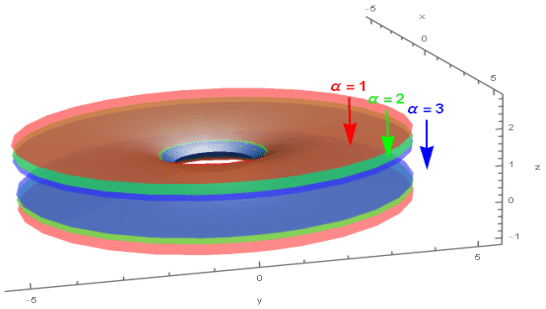


Figure 18. Embedding diagram obtained by applying the Karmakar condition for different α values and $r_0 = 1$, $C = 2$.

Also in this study, based on the solutions of the TOV equations in our two $f(R,T)$ models, we analyzed the geometry and stability of wormholes during the late evolution of the universe and concluded that the wormholes are static and stable. However, in the $f(R,T)$ model we examined in Section 4.2, due to the partial preservation of the energy conditions, the presence of exotic matter is required. We aim to investigate whether the application of the Karmarkar condition to our model in section 4.2 eliminates the need for exotic matter. In this context, we examine the evolution of the energy conditions for different values of α. The results obtained are shown in fig. 19, fig. 20, and fig. 21 (the energy conditions are examined using as $a_1 = 9\pi$ and $a_2 = -9\pi$, respectively and $C = 2$)

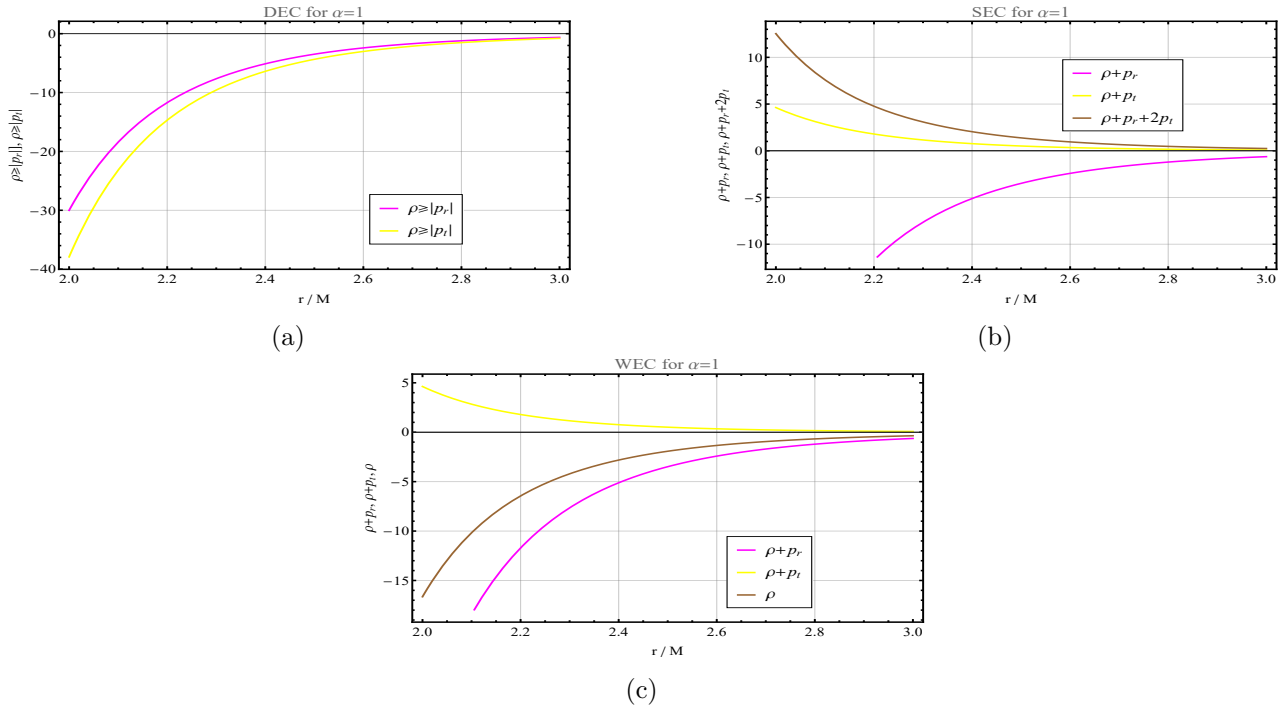


Figure 19. Karmarkar analysis of energy conditions for $\alpha = 1$. The values $r_0 = 1$, $\delta_0 = 1$, $\alpha = 1$, $M = 1$ are chosen.

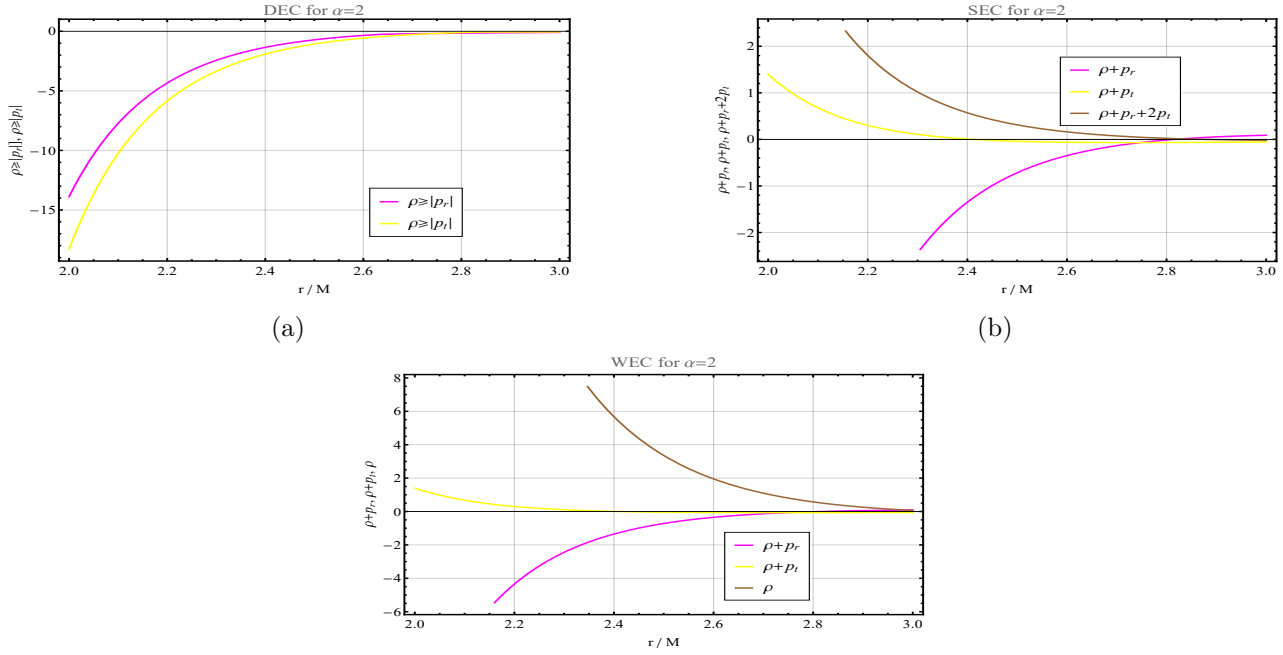


Figure 20. Karmarkar analysis of energy conditions for $\alpha = 2$. The values $r_0 = 1$, $\delta_0 = 1$, $\alpha = 1$, $M = 1$ are chosen.

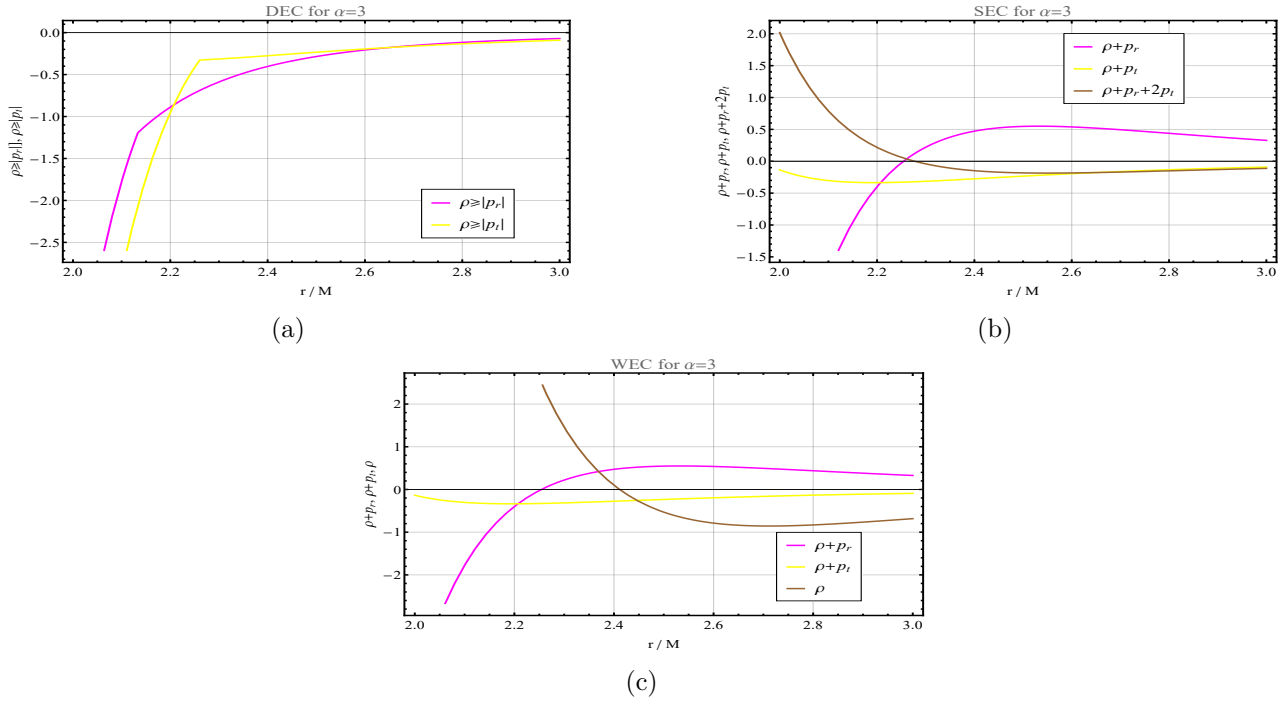


Figure 21. Karmarkar analysis of energy conditions for $\alpha = 3$. The values $r_0 = 1$, $\delta_0 = 1$, $\alpha = 3$, $M = 1$ are chosen.

6. Conclusion

In this study, we have thoroughly analyzed wormhole solutions using two well-known models [56] that generate the accelerating expansion of the universe. The dimensionless anisotropy parameter, Δ, in the wormhole model we analyzed in the presence of anisotropic matter takes negative values in both the $R - a_1^2/R + a_2T$ case 1 (Section 4.1), and the $R + a_1^2R^2 + a_2T$ case 2 (Section 4.2). This is particularly important as it indicates that the wormholes possess an attractive gravitational potential. When examining the energy conditions for case 1, as shown in Figures 5, 7, and 9, it is observed that the WEC, SEC, and Null energy conditions are satisfied, while the DEC is satisfied in the tangential pressure direction. Moreover, we analyzed the forces acting on the wormhole model and the evolution of the TOV equation for various β values in Figures 6, 8, and 10. As β values increase, the gravitational force loses its effectiveness at the throat radius $r_0 = 1$, but it becomes effective again at larger radii. Additionally, as β values increase, the hydrostatic force loses its effectiveness near the throat radius and as one moves away from the throat. However, for increasing β values, the anisotropic force, though not effective near the throat radius, takes on negative values as one moves away from the throat. According to the TOV equation, our wormhole model maintains its stable structure in all three cases, particularly around the throat region, but moves away from the static stable state as β values increase. This is thought to be due to the behavior exhibited by the anisotropic and hydrostatic forces at larger radii and with increasing β values.

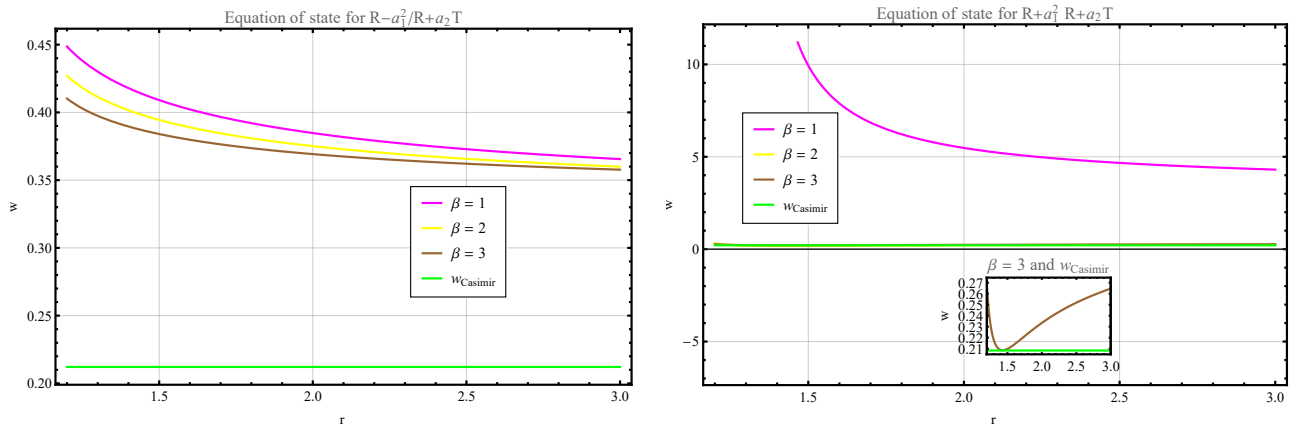
When examining the energy conditions for the case 2, as shown in Figures 12, 14, and 16, it is observed that the DEC condition is violated, while the SEC, WEC, and Null energy conditions are partially maintained. Furthermore, the evolution of the effective forces according to the TOV equation for increasing β values is examined in Figures 13, 15, and 17. Around the throat radius for $\beta = 1$, the gravitational force behaves attractively, but as the distance from the throat increases, it exhibits a repulsive character. Additionally, as the β value increases, the fluctuations in the hydrostatic and anisotropic forces become more stable. In all three β values, our wormhole model satisfies the TOV equation across all radii. It is also observed that the evolution of the energy density, ρ, is highly dependent on the value of β. As the β value increases, the energy density becomes negative. (The evolution of energy density, ρ, is shown in Figures 12, 14, and 16). This is quite an interesting situation. It is known that quantum fluctuations cause the formation of Casimir forces between two parallel conducting plates, and the magnitude of these forces increases monotonically as the distance decreases. As shown in Figure 1, the β values significantly alter the wormhole geometry. One possible explanation could be that the changing geometry generates Casimir forces, triggering the transition from positive energy (baryonic matter) to negative energy (dark matter, dark energy, or other exotic matter).

We can take a closer look at the Casimir effect. For this, our first step will be to define the equation of state of the system. The equation of state is defined as $P = w\rho$, where $P = \frac{1}{3}(p_r + 2p_t)$. Garattini (2016) has examined the properties of Casimir wormholes [80]. In light of Garattini's work, the w parameter for Casimir wormholes, denoted as $w_{casimir}$ (see equation 99, [80]), can be defined as follows

$$w_{casimir} = \frac{1}{3}\left(3 - 2\left(\frac{9r + r_0}{3r + r_0}\right)\right). \tag{6.1}$$

The graphs obtained for the two f(R,T) functions used in the paper are shown below.

For the first function (Figure 22a), we observed in our previous analyses that $\rho > 0$. Examining Figure 22a, we also see that $w > 0$. For this condition to be satisfied, $P > 0$ must hold. This condition suggests the possibility of warm dark matter. For the second function (Figure 22b), we know that $\rho < 0$. The graph located in the lower region of Figure 22b, which shows the relationship between $\beta = 3$ and $w_{casimir}$, indicates that the condition $w > 0$ is satisfied for this function. (No solution was found in the range given for $\beta = 2$ because it does not intersect with the Casimir equation of state). Examining the graph, which shows the relationship between $\beta = 3$ and $w_{casimir}$, it is understood that the equation of state parameter, w, obtained for $\beta = 3$ exhibits behavior similar to the state parameter defined for Casimir wormhole, $w_{casimir}$. Therefore, it can be concluded that specifically for $\beta = 3$ the wormhole is supported by Casimir energy around the throat radius. Here a question immediately comes to mind: can the parameters a_1 and a_2 (or any other parameters) that satisfy each energy condition individually be chosen? Theoretically, they can be selected, but in that case, the condition for the generality of the solutions would not be fulfilled.



(a) (b)

Figure 22. The relationship between the parameter w, obtained for different values of β, and the Casimir wormhole parameter $w_{casimir}$ is shown by $R - a_1^2/R + a_2T$ (a) and $R + a_1^2R^2 + a_2T$ (b). As can be seen, the w parameter for $R + a_1^2R^2 + a_2T$ is in strong agreement with the Casimir wormhole parameter $w_{casimir}$ for a specific value of the β parameter ($\beta = 3$).

In Section 4.2, the cases where the energy conditions are violated have been reexamined with the Karmarkar condition. Our aim here was also to understand the role of the shape function, which we determined through the redshift function, in the violation of energy conditions. The Karmarkar analysis also predicts the presence of exotic matter for Section 4.2. In short, when we reexamine the cases where the energy conditions are violated using the Karmarkar analysis, the need for exotic matter does not disappear (Figures 19–21).

Kavya et al. [81] demonstrated that the negative energy arising from the Casimir effect can lead to the creation of exotic matter on a small scale, which is necessary to stabilize wormholes, and their calculations have also provided evidence for the presence of positive energy near the throat region. The findings of Kavya et al. are consistent with the results presented in this article, which suggest that the wormhole geometry triggers a transformation from positive to negative energy through the influence of Casimir forces. Furthermore, Sahoo et al. [82] investigated Casimir wormholes with generalized

uncertainty principle (GUP) correction and showed that while almost no exotic matter is required to support a traversable wormhole in the absence of GUP correction, only a small amount of exotic matter is needed when the GUP correction is taken into account. The results obtained by Sahoo et al. show that the characteristic length scale introduced through GUP significantly influences the distribution of exotic matter. The assumption proposed in this study—that the variation in the radial length component also affects the matter distribution—can be evaluated on the same footing as the results of Sahoo et al. Moreover, our results are also in agreement with the study by Banerjee et al., which demonstrated that the Casimir stress energy is an ideal candidate for maintaining the stability of wormholes within the framework of $f(R,T)$ theory [83] (also see, [84]). The study by Santos et al., which demonstrated that quantum vacuum fluctuations associated with the Yang–Mills field within hadrons can provide the appropriate negative energy, is consistent with the hypothesis put forward in the present work [85].

Demonstrating that Casimir energy can play a role in the stability of wormholes supports the idea that quantum vacuum fluctuations can have a direct impact on gravitational structures. For that reason, the possibility that the wormhole geometry triggers the transition from baryonic matter to nonbaryonic matter could provide a new horizon for testing grand unified theories.

References

[1] L. Flamm, "Beitrage zur Einsteinschen Gravitationstheorie," *Phys. Z.* **17** (1916) (in German).

[2] A. Einstein and N. Rosen, "Constructing 'hair' for the three charge hole," *Phys. Rev* **48** (1935) 73-77.

[3] M. S. Morris and K. S. Thorne, "Wormholes in spacetime and their use for interstellar travel," *Am. J. Phys* **56** (1988).

[4] C. A. Picón, "On a class of stable, traversable Lorentzian wormholes in classical general relativity," *Phys. Rev. D* **65** (2002) 104010.

[5] S. Sushkov, "Wormholes supported by a phantom energy," *Phys. Rev. D* **71** (2005) 043520.

[6] F. S. N. Lobo, "Phantom energy traversable wormholes," *Phys. Rev. D* **71** (2005) 084011.

[7] O. B. Zaslavskii, " Exactly solvable model of wormhole supported by phantom energy," *Phys. Rev. D* **72** (2005) 061303.

[8] F. S. N. Lobo, "Chaplygin traversable wormholes," *Phys. Rev. D* **73** (2006) 064028.

[9] M. Jamil, P. K. F. Kuhfittig, F. Rahaman and S. A. Rakib, "Wormholes supported by polytropic phantom energy," *Eur. Phys. J. C* **67** (2010) 513.

[10] M. Jamil and M. U. Farooq, "Phantom wormholes in (2+1)-dimensions," *Int. J. Theor. Phys.* **49** (2010) 835.

[11] M. Jamil, "Evolution of a Schwarzschild black hole in phantom-like Chaplygin gas cosmologies," *Int. J. Theor. Phys.* **62** (2009) 609.

[12] M. Cataldo and F. Orellana, "Static phantom wormholes of finite size," *Phys. Rev. D* **96** (2017) 064022.

[13] F. Parsaei and S. Rastgoo, "Asymptotically flat wormhole solutions with variable equation-of-state parameter," *Phys. Rev. D* **99** (2019) 104037.

[14] P. K. F. Kuhfittig and V. D. Gladney, "A model for dark energy based on the theory of embedding," *Adv. Stud. Theor. Phys.* **12** (2018) 233.

[15] D. Wang, X. -h. Meng, "Traversable geometric dark energy wormholes constrained by astrophysical observations," *Eur. Phys. J. C* **76** (2016) 484.

[16] J. L. Blázquez-Salcedo, C. Knoll and E. Radu, "Traversable wormholes in Einstein-Dirac-Maxwell theory," *Phys. Rev. Lett.* **126** (2021) 101102.

[17] W. Israel, *Nuovo Cim. B* **144** (1966) 1.

[18] M. Visser, S. Kar and N. Dadhich, "Traversable wormholes with arbitrarily small energy condition violations" *Phys. Rev. Lett.* **90** (2003) 201102.

[19] M. La Camera, "Wormhole solutions in the Randall-Sundrum scenario," *Phys. Lett. B.* **27** (2003) 573.

[20] F. S. N. Lobo, M. A. Oliveira, "Wormhole geometries in f(R) modified theories of gravity," *Phys. Rev. D* **80** (2009) 104012.

[21] S. Capozziello, T. Harko, T. S. Koivisto, F. S. N. Lobo, and G. J. Olmo, "Wormholes supported by hybrid metric-Palatini gravity," *Phys. Rev. D* **86** (2012) 127504.

[22] J. L. Rosa, J. P. S. Lemos and F. S. N. Lobo, "Wormholes in generalized hybrid metric-Palatini gravity obeying the matter null energy condition everywhere," *Phys. Rev. D* **98** (2018) 064054.

[23] J. L. Rosa and P. M. Kull, "Non-exotic traversable wormhole solutions in linear f(R,T) gravity," *Eur. Phys. J. C* **82** (2022) 1154.

[24] M. N. Christiansen (Editor), T. K. Rasmussen (Editor), E. Anderson (Contributor), G. Basini (Contributor), S. Capozziello (Contributor) *Classical and Quantum Gravity Research*, (Nova Science Publishers, 2008).

[25] R. Garattini and F. S. N. Lobo, "Self sustained phantom wormholes in semi-classical gravity," *Classical Quantum Gravity* **24** (2007) 2401.

[26] F. S. N. Lobo, "General class of wormhole geometries in conformal Weyl gravity," *Classical Quantum Gravity* **25** (2008) 175006.

[27] R. Garattini and F. S. N. Lobo, "Self-sustained traversable wormholes in noncommutative geometry," *Physics Letters B* **671** (2009) 146.

[28] F. S. N. Lobo and M. A. Oliveira, "General class of vacuum Brans-Dicke wormholes," *Phys. Rev. D* **81** (2010) 067501.

[29] R. Garattini and F. S. N. Lobo, "Self-sustained wormholes in modified dispersion relations," *Phys. Rev. D* **85** (2012) 024043.

[30] R. Myrzakulov, L. Sebastiani, S. Vagnozzi and S. Zerbini, "Static spherically symmetric solutions in mimetic gravity: rotation curves and wormholes," *Class. Quant. Grav.* **33** (2016) 125005.

[31] T. Harko, F. S. N. Lobo, M. K. Mak and S. V. Sushkov, "Modified-gravity wormholes without exotic matter," *Phys. Rev. D* **87** (2013) 067504.

[32] L. A. Anchordoqui, S. .P. Bergliaffa and D. F. Torres, "Brans-Dicke wormholes in nonvacuum spacetime," *Phys. Rev. D* **55** (1997) 5226.

[33] B. Bhawal and S. Kar, "Lorentzian wormholes in Einstein-Gauss-Bonnet theory," *Phys. Rev. D* **46** (1992) 2464.

[34] J. Oliva and R. Troncoso, "Static wormholes in vacuum for conformal gravity," *Int. Jour. Mod. Phys. A* **24** (2009) 1528-1532.

[35] K. A. Bronnikov and S. W. Kim, "Possible wormholes in a brane world," *Phys. Rev. D* **67** (2003) 064027.

[36] F. S. N. Lobo, "General class of braneworld wormholes", *Phys. Rev. D* **75** (2007) 064027.

[37] A. G. Agnese and M. La Camera, "Wormholes in the Brans-Dicke theory of gravitation," *Phys. Rev. D* **51** (1995) 2011.

[38] K. K. Nandi, B. Bhattacharjee, S M. K. Alam and J. Evans, "Brans-Dicke wormholes in the Jordan and Einstein frames," *Phys. Rev. D* **57** (1998) 823.

[39] A. De Benedictis and D. Horvat, "On wormhole throats in f (R) gravity theory," *Gen. Relativ. Gravit.* **44** (2012) 2711.

[40] E. F. Eiroa and G. F. Aguirre, "Thin-shell wormholes with charge in F(R) gravity," *Eur. Phys. J. C* **76** (2016) 132.

[41] S. H. Mazharimousavi and M. Halilsoy, "Necessary Conditions for Having Wormholes in f(R) Gravity," *Mod. Phys. Lett. A* **31** (2016) 1650192.

[42] N. Godani and G. C. Samanta, "Traversable wormholes in f(R) with constant and variable redshift functions," *New Astron.* **80** (2020) 101399.

[43] P. Pavlovic and M. Sossich, "Wormholes in viable f(R) modified theories of gravity and weak energy condition," *Eur. Phys. J. C* **75** (2015) 117.

[44] M. Zubair, R. Saleem, Y. Ahmad and G. Abbas, "Exact wormholes solutions without exotic matter in f(R,T) gravity," *Int. J. Geom. Meth. Mod. Phys.* **16** (2019) 1950046.

[45] M. Zubair, S. Waheed and Y. Ahmad, "Static spherically symmetric wormholes in f(R,T) gravity," *Eur. Phys. J. C.* **76** (2016) 444.

[46] N. M. Garcia and F. S. N. Lobo, "Exact solutions of Brans-Dicke wormholes in the presence of matter," *Modern Physics Letters A.* **26** (2011) 3067.

[47] E. Papantonopoulos, C. Vlachos, "Wormhole solutions in modified Brans-Dicke theory," *Phys. Rev. D.* **10** (2020) 064025 .

[48] S. Dey, A. Chanda, and B. C. Paul, "Anisotropic compact objects in modified f(R,T) gravity," *arxiv e-print* (2020).

[49] T. Harko, F. S. N. Lobo, S. Nojiri and S. D. Odintsov, "f(R,T) gravity," *Phys. Rev. D.* **84** (2011) 024020.

[50] O. J. Barrientos and F. R. Guillermo, "Comment on f(R,T)," *Phys. Rev. D.* **90** (2014) 028501.

[51] P. .H R. S. Moraes and P. K. Sahoo, "Modeling wormholes in f(R,T) gravity," *Phys. Rev. D.* **96** (2017) 044038.

[52] A. K. Mishra, U. K. Sharma, V. C. Dubey and A. Pradhan, "Traversable wormholes in f(R,T) gravity," *Astrophys. Space Sci.* **365** (2020) 34.

[53] P. Sahoo, P. H. R. S. Moraes, M. M. Lapola and P. K. Sahoo, "Traversable wormholes in the traceless f(R,T) gravity," *Int. Journ. Mod. Phys. D* **30** (2021) 2150100.

[54] R. Saleem and M. I. Aslam, "Traversable wormholes in f(R,T) gravity with vanishing speed of sound," *Chinese Journal of Physics* **85** (2023) 741-751.

[55] A. Chandra, S. Dey and B. C. Paul, "Anisotropic compact objects in f(T) gravity with Finch–Skea geometry," *Eur. Phys. Jour. C.* **53** (2021) 78.

[56] J. Wu, G. Li, T. Harko and S. D. Liang, "Palatini formulation of f(R, T) gravity theory, and its cosmological implications," *Eur. Phys. Jour. C.* **78** (2018) 430.

[57] T. Harko, "Thermodynamic interpretation of the generalized gravity models with geometry-matter coupling," *Phys. Rev. D* **90** (2014) 044067.

[58] O. Bertolami and M. C. Sequeira, "Energy conditions and stability in f(R) theories of gravity with nonminimal coupling to matter," *Phys. Rev. D* **79** (2009) 104010.

[59] S. Capozziello, S. Nojiri and S. D. Odintsov, "The role of energy conditions in f(R) cosmology," *Physics Letters B* **781** (2018) 99-106.

[60] C. S. Santos, J. Santos, S. Capozziello and J. S. Alcaniz, "Strong energy condition and the repulsive character of f(R) gravity," *Gen. Rel. Gravit* **49** (2017) 50.

[61] M. Zubair and S. Waheed, "Energy conditions in f(T) gravity with non-minimal torsion-matter coupling," *Eur. Phys. J. Plus* **137** (2022) 755.

[62] N. Ganiyeva, J. L. Rosa and F. S. N. Lobo "Wormhole geometries in $f\left(R,T^2\right)$ gravity satisfying the energy conditions," *Contribution to the proceedings of the* 17*th Marcel Grossmann Meeting* (2025) .

[63] D. Roy, A. Dutta, B. Ghosh and S. Chakraborty, "Investigating Evolving Wormholes in $f(R,T)$ Gravity," *accepted paper IJMPA* (2025).

[64] M. Yousaf, and H. Asad, "Impact of modified Chaplygin gas on electrically charged thin-shell wormhole models, "*Physics of the Dark Universe* **48** (2025) 101841.

[65] M. Z. Bhatti, M. Yousaf, and Z. Yousaf, "Construction of thin-shell wormhole models in the geometric representation of f(R,T) gravity, "*New Astronomy* **106** (2024) 102132.

[66] S. Rastgoo, and F. Parsaei, "Wormholes in f(R,T) gravity with variable equation of state, "*Nuclear Physics B* **1011** (2025) 116797.

[67] S. Chaudhary, S. K. Maurya, J. Kumar and S. Kiroriwal, "Physically viable travsersable wormhole solutions and energy conditions in F(R,T) gravity within R^2 formalism via specific form of shape functions, "*Physics of the Dark Universe* **46** (2024) 101565.

[68] J. Lu, M. Xu, J. Guo, and R. Li, "Investigating the physical properties of traversable wormholes in the modified f(R, T) gravity, "*Gen. Rel. Grav.* **56** (2024) 37.

[69] T. Tangphati, A. Banerjee, and A. Pradhan, "Wormholes and energy conditions in f(R,T) gravity, "*International Journal of Geometric Methods in Modern Physics* **21** (2024) 2450109.

[70] B. R. Yashwanth, S. K. Narasimhamurthy, and Z. Nekouee, "Generalized Finslerian wormhole models in f(R,T) gravity, "*Particles* **7** (2024) 747-767.

[71] M. Mondal, and F. Rahaman, "Possible existence of galactic wormholes in f(R,T) gravity, "*Eur. Phys. J. Plus* **139** (2024) 39.

[72] H. Azmat, Q. Muneer, M. Zubair, E. Gudekli, I. Ahmad, and S. Waheed, "Class of charged traversable Casimir wormholes in f(R,T) gravity, "*Nuclear Physics B* **998** (2024) 116396.

[73] S. Chaudhary, S. K. Maurya, J. Kumar, and S. Kiroriwal, "Traversable wormhole solutions with phantom fluid in modified f(R, T) gravity, "*Pramana J. Phys.* **98** (2024) 139.

[74] M. Zubair, Q. Muneer and S. Waheed, "Energy constraints for evolving spherical and hyperbolic wormholes in f(R,T) gravity," *Eur. Phys. J. Plus* **355** (2015) 361-369.

[75] S. Mandal, P. K. Sahoo and J. R. L. Santos, "Energy conditions in f(Q) gravity," *Phys. Rev. D* **102** (2020) 024027 .

[76] E. Curiel, "A primer on energy conditions," *Einstein Studies* **13** (2017).

[77] C. Cattoen, F. Tristan and M. Visser, "Gravastars must have anisotropic pressures," *Classical Quantum Gravity* **22** (2005) 22.

[78] F. S. N. Lobo, F. Parsaei and F. N. Riazi, "New asymptotically flat phantom wormhole solutions," *Phy. Rev. D* **87** (2013) 084030.

[79] K. R. Karmarkar, *Proc. Indian Acad. Sci. A* **27** (1948) 56.

[80] R. Garattini, "Casimir wormholes," *The European Physical Journal C* **79** (2019) 11.

[81] N. S. Kavya, C. S. Varsha, L. Sudharani, and V. Venkatesha, "Unifying non-commutative geometry with Casimir energy: A novel f(R) wormhole solution," *Nuclear Physics B* **1011** (2025) 116794.

[82] A. Sahoo, S. K. Tripathy, B. Mishra, S. Ray "Casimir wormhole with GUP correction in extended symmetric teleparallel gravity," *The European Physical Journal C* **84** (2024) 325.

[83] A. Banerjee, S. Hansraj, and A. Pradhan, " Wormholes in f(R,T) gravity with casimir stress energy," SSRN, ISSN: 1556-5068 (2023).

[84] M. Zubair, S. Waheed, M. Farooq, A. H. Alkhakdi, and A. Ali, " New Casimir wormholes in f(R, T) gravity admitting conformal killing vectors," *The European Physical Journal C* **138** (2023) 902.

[85] A. C. L. Santos, R. V. Maluf, and C. R. Muniz, "Generating 4-dimensional wormholes with Yang–Mills Casimir sources," *Annals of Physics* **469** (2024) 169775